Journal Pre-proof

Complementing the intrinsic repertoire of *Ustilago maydis* for degradation of the pectin backbone polygalacturonic acid

Peter Stoffels, Markus Jan Müller, Sarah Stachurski, Marius Terfrüchte, Sebastian Schröder, Nina Ihling, Nick Wierckx, Michael Feldbrügge, Kerstin Schipper, Jochen Büchs

PII: S0168-1656(19)30910-1

DOI: https://doi.org/10.1016/j.jbiotec.2019.10.022

Reference: BIOTEC 8539

To appear in: *Journal of Biotechnology*

Received Date: 30 July 2019

Revised Date: 22 October 2019

Accepted Date: 31 October 2019

Please cite this article as: Stoffels P, Müller MJ, Stachurski S, Terfrüchte M, Schröder S, Ihling N, Wierckx N, Feldbrügge M, Schipper K, Büchs J, Complementing the intrinsic repertoire of *Ustilago maydis* for degradation of the pectin backbone polygalacturonic acid, *Journal of Biotechnology* (2019), doi: https://doi.org/10.1016/j.jbiotec.2019.10.022

Complementing the intrinsic repertoire of *Ustilago maydis* for degradation of the pectin backbone polygalacturonic acid

Running Header: Towards degradation of pectin-rich biomass by *Ustilago maydis*[1]

Peter Stoffels[a,e,#], Markus Jan Müller[b,e,#], Sarah Stachurski[b], Marius Terfrüchte[a,e], Sebastian Schröder[a], Nina Ihling[b,e], Nick Wierckx[c,d], Michael Feldbrügge[a,e], Kerstin Schipper[a,e,*] and Jochen Büchs[b,e,*]

[a] Institute for Microbiology, Cluster for Excellence on Plant Sciences, Heinrich Heine University Düsseldorf, 40204 Düsseldorf, Germany

[b] Aachener Verfahrenstechnik – Biochemical Engineering, RWTH Aachen University, Forckenbeckstr. 51, 52074 Aachen, Germany

[c] iAMB - Institute of Applied Microbiology, ABBt - Aachen Biology and Biotechnology, RWTH Aachen University, Worringerweg 1, 52074 Aachen, Germany

[d] Institute of Bio- and Geosciences IBG-1: Biotechnology, Forschungszentrum Jülich, Wilhelm-Johnen-Str., 52425 Jülich, Germany

[e] Bioeconomy Science Center (BioSC), c/o Forschungszentrum Jülich, 52425 Jülich, Germany

[#] The authors contributed equally.

[*] Corresponding authors:

Dr. Kerstin Schipper, Heinrich Heine University Düsseldorf, Institute for Microbiology, Bldg. 26.12.01.64, 40204 Düsseldorf, Germany; Phone: +49 (0) 211 - 81-10451; Fax: +49 (0) 211 - 81-15370; E-mail: kerstin.schipper@uni-duesseldorf.de.

Prof. Dr.-Ing. Jochen Büchs, RWTH Aachen University, Aachener Verfahrenstechnik – Biochemical Engineering, Bldg. NGP2/A-307, Forckenbeckstr. 51, 52074 Aachen, Germany; Phone: +49 (0) 241 - 80-23569; Fax: +49 (0) 241 80 22635; E-mail: jochen.buechs@avt.rwth-aachen.de

Highlights

- Compilation of detailed inventory of intrinsic pectinolytic enzymes of U. maydis
- Activation of intrinsic endo-polygalacturonase in the yeast form
- Complementation of the pectinolytic repertoire by bacterial and fungal enzymes
- Online evaluation method for enzymatic substrate degradation using respiratory data
- Co-fermentation of engineered strains for efficient growth on polygalacturonic acid

Abstract

Microbial valorization of plant biomass is a key target in bioeconomy. A promising candidate for consolidated bioprocessing is the dimorphic fungus *Ustilago maydis*. It harbors hydrolytic enzymes to degrade biomass components and naturally produces valuable secondary metabolites like itaconic acid, malic acid or glycolipids. However, hydrolytic enzymes are mainly expressed in the hyphal form. This type of morphology should be prevented in industrial fermentation processes. Genetic activation of these enzymes can enable growth on cognate substrates also in the yeast form. Here, strains were engineered for growth on polygalacturonic acid as major component of pectin. Besides activation of intrinsic enzymes, supplementation with heterologous genes for potent enzymes was tested. The presence of an unconventional secretion pathway allowed exploiting fungal and bacterial

enzymes. Growth of the engineered strains was evaluated by a recently developed method for online determination of residual substrates based on the respiration activity. This enabled the quantification of the overall consumed substrate as a key asset for the assessment of the enzyme degradation potential even on polymeric substrates. Co-fermentation of endo- and exo-polygalacturonase overexpression strains resulted in efficient growth on polygalacturonic acid. In the future, the approach will be extended to establish efficient degradation and valorization of pectin.

Abbreviations

CAZyme, carbohydrate-active enzyme; CM, complex medium; CTR, carbon dioxide transfer rate; DNS, 3,5-dinitrosalicylic acid; ER, endoplasmic reticulum; f. c., final concentration; GH, glycoside hydrolase; Gus, β-glucuronidase; HG, homogalacturonan; n.s., not significant; OD_{600}, optical density (600 nm); OTR, oxygen transfer rate; RAMOS, respiration activity monitoring system; RGI / RGII, rhamnogalacturonan I / II; RQ, respiratory quotient; RT, room temperature; XG, xylogalacturonan.

Keywords: CAZyme, co-fermentation, oxygen transfer rate, polygalacturonic acid, unconventional secretion, *Ustilago maydis*

1. Introduction

One key step towards a sustainable bioeconomy is the transition away from fossil resources to the synthesis of chemicals or chemical building blocks from renewable bio-based substrates, waste materials, or low-value industrial by-products (1, 2). Sugar beet pulp is an abundant but low-value by-product of the sugar industry which accumulates during sugar production in Europe and the United States. Worldwide about 8.6 million metric tons of dried fiber-rich sugar beet pulp are used as animal feed (web reference 1). However, the economic profit is limited due to the drying costs (3). Hence, it would be advantageous to use sugar beet pulp for production of high-value substances in a microbial consolidated bioprocess. Substrate

costs of 123 US$ / t of sugar beet pulp dry matter (web reference 2) and a market price of 1500 US$ / t for itaconic acid (4) as a potential product indicate the economic range for the microbial conversion of sugar beet pulp. The respective microorganisms must be able to enzymatically hydrolyze the (pretreated) pectin-rich pulp to release fermentable sugars and, at the same time, produce a valuable product.

Four structural classes of pectic polymers exist: homogalacturonan (HG), rhamnogalacturonan I (RGI), xylogalacturonan (XG), and rhamnogalacturonan II (RGII). HG and RGI are depicted in Fig. 1. HG is composed of partially esterified polygalacturonic acid, an α-1,4-linked galacturonic acid (galacturonic acid) polymer (5, 6). RGI, RGII and XG consist of a heteropolymer backbone and several different side chains including numerous different sugars (5). Due to its complex structure, a large set of carbohydrate-active enzymes (CAZymes) is needed for efficient pectin degradation (7). HG represents the most abundant structural class with a share of about 60% (w/w) (8). Complete HG degradation requires the efficient interplay of exo- and endo-polygalacturonases that in concert hydrolyze the polygalacturonic acid backbone. Alternatively, pectate and pectin lyases can break the α-1-4 bonds by a trans-elimination mechanism yielding unsaturated (methyl)oligogalacturonates (9). In addition, methyl-esterifications and *O*-acetylations of the polygalacturonic acid backbone result in the additional need for pectin methylesterases and pectin acetylesterases (10). Hydrolysis of other structural classes containing, among others, arabinose, rhamnose, galactose, fucose and xylose moieties, requires diverse other hydrolytic enzymes (5).

A multitude of pectinolytic enzymes is produced by ascomycete filamentous fungi like *Aspergillus niger* (11), basidiomycete mushrooms like *Schizophyllum commune* (12) and various bacteria (7). Potent enzymes can be heterologously produced in *Saccharomyces cerevisiae* and are currently used in different industrial applications, with fruit juice extraction and clarification as the most important process (13).

With respect to consolidated bioprocessing, recent research has focused on converting the established fungal model *S. cerevisiae* into a host for bioethanol production from pectin. *S. cerevisiae* does not produce intrinsic CAZymes for biomass degradation and does not naturally grow on many of the pectin components like galacturonic acid. Therefore, genetic engineering for substrate hydrolysis and uptake was conducted (14, 15). Another study describes the expression of an endo-polygalacturonase in *S. cerevisiae*, but the aim was not on substrate consumption (16). To our knowledge, no efficient process using *S. cerevisiae* simultaneously as CAZyme production host and for galacturonic acid metabolization has been published yet. As mentioned above, some filamentous fungi are naturally equipped for pectin degradation and hence constitute promising alternatives to the yeast system (17). However, suitable high-value products are lacking and efficient culturing in bioreactors remains a challenge (18, 19).

In the past years, the corn smut fungus *Ustilago maydis* has emerged as an attractive candidate for consolidated bioprocessing (20, 21). The basidiomycete is mostly known for its ability to cause corn smut disease in its host maize and has been studied for decades. By now, it has developed into a fungal model that is prominent for research on host-pathogen interaction, cell and RNA biology as well as homologous recombination (22, 23). Handling of *U. maydis* in the laboratory is very well established and includes a versatile toolset for efficient genetic manipulation yielding genetically stable strains (24-28). The duplication time is less than two hours in the presence of glucose as sole carbon source (21, 30). The dimorphic fungus can be grown in the laboratory in a haploid yeast form that duplicates by budding. These haploid cells are very robust and, in contrast to filamentous fungi, can easily be cultivated in submerged culture, including large-scale cultivation in bioreactors (18, 29). In nature, after mating of compatible yeast cells, infectious hyphae are formed that penetrate the plant surface and cause infection (31). However, pure axenic cultures of haploid cells without a suitable mating partner are considered harmless, and since the crucial genetic factors for

infection like the mating genes are known, the fungus can easily be transformed into a non-infectious, safe-to-use form (21, 32). In submerged culture of haploid cells, a morphological switch to hyphal growth can also occur under the influence of stresses such as low pH or nutrient limitations (33), but this switch can be avoided through disruption of the mitogen-activated protein kinase (MAPK) signal transduction pathway that regulates the sexual cycle (34). Such a modification does not affect the fitness of the cell under biotechnologically relevant conditions (35). Of note, *U. maydis* has a very narrow host range infecting only *Zea mays* and its ancestor Teosinte. It is innocuous to humans and infected plant parts are even relished as a delicacy called *Huitlacoche* in Central America (21, 36).

From a biotechnological perspective, *U. maydis* is very interesting because it naturally produces valuable secondary metabolites, including organic acids like itaconic and malic acid as well as the glycolipids ustilagic acid and mannosylerythrytol lipids (37-41). As a plant pathogen, *U. maydis* also contains a limited but potent set of conventionally secreted hydrolytic enzymes including several CAZymes such as multiple xylanases, endoglucanases, β-glucosidases and oxidoreductases (20, 42-46). Hence, it would be perfectly suited for biomass valorization. Unfortunately, the CAZymes are mainly produced during the infections stage in the plant and not during the biotechnologically relevant yeast phase (42). We recently addressed this problem and activated several CAZymes in the yeast phase by exchanging the native promoters of the respective genes by a strong artificial promoter (47). This enabled the secretion of active enzymes during yeast-like growth and resulted in degradation of novel simple biomass-related substrates like cellobiose (20). Additionally, as a proof of principle, itaconic acid was produced using cellobiose as sole carbon source (20).

U. maydis not only harbors the conventional secretion pathway for protein export via the endomembrane system but also an unconventional secretion route (48, 49). Chitinase Cts1 has been identified as a target protein that is exported via the fragmentation zone of dividing cells in a novel lock-type mechanism (49-51). Export of heterologous proteins via unconventional

secretion using Cts1 as a carrier has been established a few years ago (28, 52, 53). Importantly, unconventional secretion circumvents the endomembrane system and consequently the cognate post-translational modifications. This can be essential for secretion of bacterial proteins coincidentally containing detrimental eukaryotic *N*-glycosylation sites (28, 50).

U. maydis is able to grow on monomeric galacturonic acid, the most abundant sugar in pectin, as we have shown recently in a parallel methodological study (54). This ability has been proven by application of the respiration activity monitoring system (RAMOS), enabling the development of a methodology for the online quantification of consumed galacturonic acid. It is based on the stoichiometric linkage between galacturonic acid consumption, oxygen consumption and carbon dioxide release. Extension of this methodology towards polymeric substrates even enabled the determination of enzymatic activity in the culture supernatant (54). Thus, the RAMOS technology provides a powerful tool for the characterization of CAZyme producing strains based on their metabolic activity on complex substrates.

In this work we extended our previous approach of activating intrinsic CAZymes for the degradation of plant biomass components (20) to perform the first important step towards valorization of pectin-rich biomass. We focused on the major pectin component, polygalacturonic acid, and used a combination of genetic methods and bioprocess engineering to establish its decomposition and consumption. By application of online monitoring tools, we compared the hydrolytic activity of different intrinsic and heterologous polygalacturonases on polygalacturonic acid. To assess additive effects, we co-cultivated *U. maydis* strains expressing endo- and exo-polygalacturonase and identified a suitable combination for complete substrate conversion.

2. Materials and methods

2.1 Plasmids, strains and media

All plasmid vectors were generated using standard molecular cloning methods including Golden Gate cloning (25, 55). Plasmids were propagated in *Escherichia coli* Top10 cells. The vector for intrinsic gene activation with the strong P_{oma} promoter was assembled by Golden Gate cloning (20, 25) using approximately 1 kb flanking regions in the 5´ region of the intrinsic open reading frame thereby deleting the putative region for the native promoter of about 1 kb. Genomic DNA of *U. maydis* strain UM521 (56) was used as a template for flank generation by PCR (web reference 4). Heterologous genes were inserted in the *ip* locus using integrative vectors mediating carboxin resistance (28) or in the modified *upp3* locus of strain AB33P5ΔR, in which 5 proteases including *upp3* had previously been sequentially deleted (52). Heterologous genes were specifically codon-optimized for expression in *U. maydis* using an online tool (57, 58) and produced by chemical gene synthesis (Integrated DNA Technologies, Leuven, Belgium). Oligonucleotides used for molecular cloning are listed in Table 1.

pUMa2822 (pDest_Poma:umag_02510_NatR) for *in locus* promoter exchange of *umag_02510* was generated by SapI-mediated Golden Gate cloning. The reaction included the up- and downstream flanks generated on UM521 gDNA using the primer combinations MF425xMF426 and MF427xMF428, respectively, the storage vector pUMa2443 (51) containing a nourseothricin resistance cassette (NatR) and the P_{oma} promoter, as well as the destination vector pUMa2074 (51). The integrative plasmids for insertion at the *ip* locus pUMa3108 (pRabX1_Poma_pgaX_CbxR), pUMa3400 (pRabX1_Poma_pguB-cts1_CbxR), pUMa3401 (pRabX1_Poma_peh1-cts1_CbxR), pUMa3403 (pRabX1_Poma_pga1_CbxR) were generated by standard restriction-ligation cloning. The corresponding codon-optimized heterologous genes were synthetized with cognate flanking restriction sites. Heterologous

fungal genes included their N-terminal native signal peptides for entry of the Endoplasmic Reticulum (ER) whereas the signal peptides of bacterial genes were eliminated for export of the corresponding protein by Cts1-mediated unconventional secretion (signal peptides predicted with SignalP5.0; web reference 5) (59). pUMa2113 (52) served as backbone for insertion of bacterial genes via NcoI/SpeI or BamHI/SpeI sites, thereby replacing the *gus* gene, resulting in translational Cts1 fusions. For insertion of fungal genes, pUMa2113 was modified removing *cts1* via NotI/SfiI and NcoI/SfiI hydrolysis creating an intermediate vector carrying the P_{oma} promoter (47) and the *gus* gene fused to a SHH-tag encoding sequence which consists of a OneStrep, 3x HA and a 10x His tag (52). The construct was inserted at the *ip* locus, which is an established locus for the expression of heterologous genes (28). Via restriction with BamHI/SfiI the *gus* gene was removed from the intermediate vector and replaced by the respective heterologous fungal gene upstream (*in frame*) of the *shh* sequence (52). Plasmid sequences and detailed cloning strategies will be provided upon request.

U. maydis strains applied or generated in this study are listed in Table 2. Genomically stable strains were obtained by homologous recombination using the parental strain AB33P5ΔR (52). All plasmids were linearized at the flank borders or within the ip^R allele using unique restriction endonucleases (25, 60). Excised linear constructs were used to transform *U. maydis* protoplasts (60). Each genetic modification was verified by Southern blot analysis using digoxigenin labeled probes (PCR Dig Labeling Mix, Roche, Basel, Switzerland). Mutants transformed with integrative plasmids were selected for harboring a single plasmid copy in the *ip* locus by Southern blot analysis using a probe generated by PCR using primer combination MF502/MF503 and the template pUMa260 (61). For *in locus* modifications the complete flanking regions were used as probes.

For strain generation *U. maydis* strains were grown at 28°C in complete medium (CM) supplemented with 10 g/L glucose (CM-Glc) (63). For determination of enzyme activities indicated strains were grown at 28°C in modified Verduyn mineral medium (4 g/L NH_4Cl,

0.2 g/L $MgSO_4 \times 7\ H_2O$, 0.1 g/L $FeSO_4 \times 7\ H_2O$, 0.5 g/L KH_2PO_4, 1.0 mL/L trace element solution, 0.1 M MES buffer, pH 6.0; trace element solution: 15.0 g/L EDTA, 4.5 g/L $ZnSO_4 \times 7\ H_2O$, 4.5 g/L $CaCl_2 \times 2\ H_2O$, 3.0 g/L $FeSO_4 \times 7\ H_2O$, 1.0 g/L H_3BO_3, 0.84 g/L $MnCl_2 \times 2\ H_2O$, 0.33 g/L $CoCl_2 \times 6\ H_2O$, 0.3 g/L $CuSO_4 \times 5\ H_2O$, 0.4 g/L $Na_2MoO_4 \times 2\ H_2O$, 0.1 g/L KI) (54). The modified Verduyn mineral medium was supplemented with 1% (w/v) glucose unless stated otherwise.

2.2 Bioinformatic evaluation

To identify *U. maydis* orthologues of *Aspergillus niger* enzymes acting in galacturonic acid catabolism, respective amino acid sequences were subjected to BlastP analyzes on the National Center for Biotechnology Information (NCBI) server. *U. maydis* 521 (taxid:237631) served as a reference protein dataset (web reference 6). Amino acid identities over the whole length of homologous sequences were determined by amino acid alignments using the program CloneManager 12 (Sci-Ed Software).

Putative enzyme functions and GH domains of pectinolytic enzymes were derived from BlastP analyzes against the full reference protein database (refseq_protein) on NCBI. Well-characterized proteins upon the top hits were used for amino acid alignments and conservation of functional residues was determined based on available literature information. N-terminal signal sequences for prediction of conventional secretion were determined by SignalP4.1 (web reference 7) (59). *U. maydis* amino acid (umag) sequences were retrieved from the EnsemblFungi *U. maydis* genome homepage (web reference 4). The amino acid alignment has been assembled using Clustal Omega (web reference 8) (64) and the program ESPript 3.0 (65).

2.3 Preparation of cell extracts

U. maydis cell extracts were prepared as described in Stock *et al.* 2016 (66) using denaturing sodium phosphate buffer (0.1 M Na_2HPO_4/NaH_2PO_4, 8 M Urea, 0.01 M Tris/HCL,

pH 8.0) supplemented with a protease inhibitor mix (1 mM phenylmethylsulfonylfluorid (PMSF), 10 mM DTT, 2.5 mM benzamidine hydrochloride hydrate, 5 × cOmplete Protease EDTA-free Protease Inhibitor Cocktail (Sigma-Aldrich, now Merck, Darmstadt, Germany). Cell pellets of 2 mL cultures were mixed with 500 µL of denaturing sodium phosphate buffer and 100 µL of glass beads (0.25-0.5 mm; Carl Roth, Karlsruhe, Germany). The cell disruption was performed in a ball mill (Retsch, Haan, Germany) at 30 Hz for 5 min. The mixture was centrifuged at 16,000 × *g* for 30 min. 400 µL of the supernatant were transferred to a new 1.5 mL reaction tube and stored on ice. The protein concentration of the supernatant was determined via Bradford assay. 10 ng of protein was incubated with 1 × denaturing Laemmli-buffer (67) in a volume of 20 µL at 95°C for 10 min. For subsequent deglycosylation of cell extracts, the denaturation of the protein was performed in 1 × glycoprotein reaction buffer (see below).

2.4 Protein precipitation from culture supernatants

To precipitate proteins, cell free culture supernatants were harvested by centrifugation (16,000 × g, 10 min) and supplemented with 10% (v/v) trichloric acid (TCA). After overnight incubation at 4°C, precipitates were pelleted by centrifugation (16,000 × g, 30 min, 4°C) and washed twice with ice-cold acetone (precooled to -20°C). The protein pellets were then resuspended in 15 µL of 3 × denaturing Laemmli-buffer (67) (protein concentration factor about 60 ×) and the pH was neutralized with 2 µL 1 M NaOH. For SDS-Page analysis, the samples were boiled for 10 min. After centrifugation (22,000 × g, 5 min, room temperature (RT)) the supernatants were used for SDS-Page.

2.5 SDS-Page and Western blot analysis

SDS-Page was used to separate proteins by their molecular masses. Proteins from gels were transferred to methanol-activated PVDF membranes using semi-dry Western blotting. Tagged proteins were detected using primary anti-HA antibodies (Sigma-Aldrich, now

Merck, Darmstadt, Germany; 1:3,000 dilution) and secondary anti-mouse IgG-HRP conjugates (Promega, Mannheim, Germany; 1:4,000 dilution). Blots were developed using AceGlow Western blotting detection reagent (PeqLab, now VWR, Erlangen, Germany) and a LAS4000 chemiluminescence imager (GE LifeScience/VWR, Erlangen, Germany). To visualize protein loading, the PVDF membranes were stained with Coomassie Brilliant Blue by a 5 minute incubation step in the staining solution (0.05% Coomassie Brilliant Blue R250, 15% (v/v) acetic acid, 15% (v/v) methanol), followed by a short rinse in water and subsequent drying.

2.6 Protein deglycosylation

Proteins in cell extracts or precipitated culture supernatants were treated with the PNGaseF deglycosylation kit (New England Biolabs, Frankfurt am Main, Germany) to remove the sugar moieties of *N*-glycosylations. 10 µg of cell extracts or protein pellets obtained by TCA precipitation were dissolved in 10 µL 1 × glycoprotein reaction buffer and denatured by incubation at 95°C for 10 min. 2 µL 10% (w/v) Nonidet P-40 (NP-40), 2 µL 10 × GlycoBuffer II and 1 µL PNGaseF were added and the volume adjusted to 20 µL with H_2O. Reaction mixes were incubated for 4 h at 37 °C and subsequently analyzed by SDS-Page and Western blot analysis.

2.7 Offline polygalacturonase activity assays

Enzymatic activity of exo- and endo-polygalacturonases in cell free culture supernatants was determined using dinitrosalicylic acid (DNS) assay (68) as described for other substrates (20). Therefore, shake flask cultures (100 mL shake flasks) of respective strains were inoculated in 10 mL of modified Verduyn mineral medium containing 10 g/L glucose at an optical density (OD_{600}) of 0.5 and incubated for 24 h (Infors shaker HT Ecotron, 200 rpm, shaking diameter 50 mm, 28°C). At this time glucose was completely consumed, which was initially verified by DNS assays (Table S1) or roughly estimated by glucose test strips

(detection range of 0.5 g/L to 10 g/L; Macherey-Nagel, Düren; Germany). Supernatants were then collected in 2 mL reaction tubes by centrifugation (3 min, 16,000 × g, RT). 200 µL culture supernatant was mixed with 800 µL polygalacturonic acid solution (0.5% (w/v) polygalacturonic acid, purity 85% [Carl Roth, Karlsruhe, Germany] in 0.1 M sodium acetate buffer, pH 5.5) and incubated at 30°C (600 rpm). 60 µL samples were taken at 0, 6 and 24 h and incubated at 95°C for 10 min to deactivate the respective enzymes. Samples were stored at -20°C until the DNS assay was performed. For the colorimetric reaction, the samples were thawed at room temperature, mixed with 60 µL of DNS reagent (10 g/L 3,5-dinitrosalicylic acid (Sigma-Aldrich, now Merck, Darmstadt, Germany), 404 g/L sodium potassium tartrate tetrahydrate, 0.4 M sodium hydroxide) and incubated at 95°C for 10 min to facilitate the reaction from 3,5-dinitrosalicylic acid to 3-amino-5-nitrosalicylic acid, resulting in a color shift from yellow to red. Next, reaction mixes were cooled to RT and centrifuged for 1 min at 16,000 × g to sediment the remaining polygalacturonic acid. 80 µL of each sample was loaded onto transparent polystyrol 96-well microtiter plates (Greiner Bio-One, Frickenhausen, Germany). Absorption was determined at 540 nm using a Tecan 200 plate reader (Tecan, Männerdorf, Switzerland). In order to quantify the amount of released galacturonic acid, a standard curve was recorded using standard solutions with concentrations of 0, 0.625, 1.125, 2.5, 5.0, 10.0 and 20.0 mM of galacturonic acid. Initial values (0 h) were subtracted to remove background.

2.8 Online measurement of the metabolic activity

Online monitoring of the oxygen transfer rate (OTR), the carbon dioxide transfer rate (CTR) and the respiratory quotient (RQ) enabled determining the metabolic activity of cultures. Cultivations were performed in modified 250 mL shake flasks using an in house built respiration activity monitoring system (RAMOS) (69, 70). Commercial versions of the device are available from Kühner AG (Birsfelden, Switzerland) or HiTec Zang GmbH (Herzogenrath, Germany). The flasks were filled with 20 mL modified Verduyn mineral

medium (ref. section 2.1) that was inoculated with an over-night grown pre-culture to an initial OD_{600} of 0.6 and shaken in a ISF1-X shaking incubator (Kühner AG, Birsfelden, Switzerland) at 30°C with a shaking frequency of 300 rpm at a shaking diameter of 50 mm. As carbon sources, the medium was supplemented with 4 g/L glucose and varying amounts of (poly)galacturonic acid. Consumption of (poly)galacturonic acid leads to an increasing pH. To prevent alkalization during growth on those acid substrates, the buffer type and concentration was changed from 0.1 M MES, pH 6.0 (ref. section 2.1) to 0.2 M MOPS, pH 6.0.

Based on the respiratory quotient (RQ), cultivation phases with glucose and (poly)galacturonic acid consumption were identified, as described previously (54). Polygalacturonic acid consumption started after the OTR and RQ drop due to glucose depletion. The end of polygalacturonic acid consumption was defined as the time point where a linear fit of the RQ reached a value of 1.2. This value corresponds to the theoretical RQ value for pure combustion of (poly)galacturonic acid. Fig. S2 depicts an exemplary fit of the RQ during the cultivation represented in Fig. 9. The overall consumed oxygen during consumption of (poly)galacturonic acid, calculated as the integral of the OTR curve, was used to estimate the respective residual substrate concentration (54). The enzymatic activity in the culture supernatant was determined from the linear decrease of the calculated concentration of residual (poly)galacturonic acid over time (54).

2.9 Offline analytics

For offline sampling, cotton plug-sealed shake flasks were cultivated in parallel to the RAMOS flasks under identical cultivation conditions. The pH value of unfiltered culture broth was measured at RT using a HI2211 pH meter (Hanna Instruments, Vöhringen, Germany). Glucose and galacturonic acid concentrations were determined from cell-free supernatant. After sterile filtration with 0.2 µm filters (Rotilabo syringe filters Mini-Tip cellulose acetate membrane, N° PP52.1, Carl Roth, Karlsruhe, Germany), the samples were

separated by HPLC using an organic acid resin column (250 x 8 mm, CS-Chromatographie Service GmbH, Langerwehe, Germany). The separation was achieved with 1 mM H_2SO_4 at 75 °C and a flow rate of 0.8 mL/min. The column was coupled to a refractometer and the data was analyzed by the software Chromeleon 6.2 (Dionex, Germering, Germany).

2.10 Determination of liberated galacturonic acid during RAMOS cultivations

The overall liberated amount of galacturonic acid was determined using the following calculations:

$$GalA_{lib} = GalA_{sup} + GalA_{con} \quad (1)$$

$GalA_{lib}$: concentration of overall liberated galacturonic acid from polygalacturonic acid [g/L]

$GalA_{sup}$: concentration of galacturonic acid in the culture supernatant, measured by HPLC [g/L]

$GalA_{con}$: concentration of the overall consumed galacturonic acid [g/L], determined from the integral of the OTR curve as described earlier (54)

The liberation rate of galacturonic acid between two sampling time points (t_1 and t_2) can be calculated by:

$$\frac{\Delta GalA_{lib}}{\Delta t} = \frac{GalA_{lib,2} - GalA_{lib,1}}{t_2 - t_1} \quad (2)$$

This liberation rate was plotted against $t = \frac{t_1 + t_2}{2}$.

2.11 Microscopic analyses

For microscopy, cells were immobilized on agarose patches (2% final concentration (f. c.)). Life/dead staining was performed using propidium iodide. The strains were cultivated as described for the online measurements above and samples were taken after 8 and 36 h of

cultivation time. For staining the samples, 150 µL of cell suspension were incubated for 10 min with 0.6 µL of aqueous propidium iodite solution (1 µg/µL) on a Vibrax VXR Basic laboratory shaker (IKA® -Werke GmbH & CO. KG, Staufen, Germany). A wide-field microscope setup from Visitron Systems, Axio Imager M1 (Visitron Systems GmbH, Puchheim, Germany) equipped with a CCD camera and the objective lens Plan Neofluar (40 x, NA 1.3; 63 x, NA 1.25) (Carl Zeiss, Jena, Germany) was used. The propidium iodite signal was acquired using a HXP metal halide lamp (LEj, Jena, Germany) in combination with a filter set for Rfp/mCherry (ET560/40BP, ET585LP, ET630/75BP). The microscopic system was controlled by the MetaMorph software (Molecular Devices, version 7, Sunnyvale, USA). The program was also used for adjustment of brightness and contrast for image processing.

3. Results and discussion

3.1 Inventory of intrinsic enzymes for pectin degradation and metabolization

Earlier studies suggested that some pectinolytic enzymes are present in *U. maydis* (42, 43, 45, 56). To inspect its natural abilities to degrade pectin in more detail, a list of potentially relevant enzymes was collected and carefully re-evaluated bioinformatically. Therefore, the proteins were inspected for the presence of enzymatic domains, especially of glycoside hydrolase (GH) domains and conserved domains of other CAZyme families (web reference 3) (71). Furthermore, a screening for conventional N-terminal secretion signals (SignalP5.0; web reference 5) was performed, and well-characterized orthologues were identified by BlastP analysis to compare enzyme architectures and the presence of active site residues (Fig. 1; Table S2).

The analysis confirmed that several potential secreted pectinolytic enzymes with conserved hydrolytic domains are encoded in the *U. maydis* genome. These include a putative endo-polygalacturonase, pectin lyase and pectin methylesterase. These enzymes are potentially

acting on the polygalacturonic acid backbone in HG (Fig. 1, Fig. S1; Table S2). For example, the putative endo-polygalacturonase shows homology to well-characterized endo-polygalacturonases like the ones from *Fusarium moniliforme* and *Aspergillus aculeatus*. Substrate binding sites and residues involved in proton donation to the glycosidic oxygen and activation of H_2O for the nucleophilic attack are conserved (Fig. 2) (72, 73). In addition it carries a predicted N-terminal signal peptide for secretion via the conventional endomembrane system (Fig. 2; Table S2), which is in line with its putative extracellular function.

In addition to the enzymes acting on HG, three putative arabinofuranosidases and two arabinases were detected in the *U. maydis* genome. Those enzymes break down arabinofuranose or arabino-oligosaccharides from RG I and II side chains. Finally, other enzymes were identified which act on less abundant sugar residues (e.g., β-galactosidase; Fig. 1; Table S2).

As described before, pectinolytic enzymes are mainly secreted during plant infection and not during the biotechnologically relevant yeast stage (42). This finding is in line with our earlier observation that in the yeast form the fungus is not even able to grow naturally on the polygalacturonic acid backbone of pectin (54). By contrast, an earlier study reported growth of similar *U. maydis* wild type strains on polygalacturonic acid (45), a contradictory observation that cannot be explained to date but might be attributed to the source and purity of the substrate .

Most enzymes acting on the HG backbone release galacturonic acid, the main building block of pectin. Galacturonic acid also represents the major component of pectin hydrolysates (8). Therefore, the metabolization of this monosaccharide is a prerequisite for growth on pectin. To evaluate the ability of *U. maydis* to consume galacturonic acid, the bioinformatics survey was extended. A conserved catabolic pathway of galacturonic acid has been described in *Aspergillus niger* and other filamentous fungi (74). It involves enzymes that convert

galacturonic acid into pyruvate and L-glyceraldehyde in three enzymatic steps. L-glyceraldehyde is subsequently reduced to glycerol. To identify homologs in *U. maydis*, BlastP analyses using the enzyme amino acid sequences from *A. niger* (75) as queries were applied. Homologs of all four enzymes are encoded in the *U. maydis* genome, ranging between 38 and 60% amino acid identity (Fig. 3). This suggests that *U. maydis* is able to catabolize galacturonic acid via a similar pathway like *A. niger*. By contrast, the central regulator GaaR for galacturonic acid utilization in *A. niger* is not clearly conserved in *U. maydis (76)*, leaving the regulation of the pathway open.

In summary, the bioinformatic analyses indicated that *U. maydis* is able to grow on galacturonic acid and contains enzymes to hydrolyze some of the enzymatic bonds in pectin molecules. However, the present enzyme set is clearly not sufficient to completely degrade the complex polymer into its monomers, because essential players are lacking for HG degradation, e.g., exo-polygalacturonase and pectin acetylesterase (Fig. 1). It is thus likely that as a biotrophic *U. maydis* does not feed on pectin but instead uses the present enzymes to loosen the recalcitrant structure of the plant cell walls for penetration during in planta growth (42). Deletion of the genes for predicted endo-polygalacturonase, pectin lyase or pectin methyl-esterase did not impair virulence, suggesting that the function of the enzymes during plant infection is dispensable (42).

3.2 Activation of an intrinsic endo-polygalacturonase

As a first step towards degradation of the polygalacturonic acid backbone of pectin, we focused on the activation of intrinsic enzymes during the yeast phase. Initially, an overexpression strain of the most important intrinsically encoded enzyme acting on pure polygalacturonic acid, the predicted endo-polygalacturonase (UmPgu1; encoded by *umag_02510*; Fig. 1 and Fig. 2), was generated using an established promoter exchange strategy. Here, the native promoter of the respective gene is replaced by the strong, constitutive P_{oma} promoter (Fig. 4A) (20). The construct was stably introduced in the protease-

deficient strain AB33P5ΔR. This strain lacks a total of five proteases and has a significantly reduced proteolytic activity in the culture supernatant, thus, avoiding possible extracellular degradation of the secreted enzyme (52). The morphology of the engineered strain was not impaired (Fig. S3). To check for enzyme activity, cell-free culture supernatant of the expression strain AB33P5ΔR/UmPgu1 was incubated with the substrate polygalacturonic acid. In contrast to the progenitor strain, the supernatant of the activated strain caused a significant increase in reducing groups released from polygalacturonic acid, as detected by DNS assay (Fig. 4B). This confirms the bioinformatics prediction that UmPgu1 is indeed an active secreted polygalacturonase.

3.3 Complementation with unconventionally secreted heterologous bacterial polygalacturonases

Since the genome of *U. maydis* does not encode a complete enzyme set for pectin degradation and especially lacks any obvious exo-polygalacturonase homologue for release of monomeric galacturonic acid from polygalacturonic acid, we aimed on testing complementation with potent heterologous enzymes. The ability to secrete potent bacterial enzymes is a unique opportunity of our system. It is only feasible because of the existence of the unconventional lock-type secretion pathway (Fig. 5A) (51), which circumvents the endomembrane system and, thus, potentially harmful posttranslational modifications (28).

We started out using exo-polygalacturonase PguB from *Klebsiella sp. CGMCC 4433* (KpPguB; accession number **JQ388228.1**; GH28), a potent bacterial enzyme that has been described to match the physiological requirements of UmPgu1 (77). To this end, a strain in which a codon-optimized version of the respective gene was expressed as translational fusion with the carrier Cts1 for unconventional secretion was generated (Fig. 5B) (28). Of note, the sequence for the native signal peptide present in the bacterial gene was eliminated to redirect it to the unconventional secretion pathway.

Western blot analyses demonstrated that the fusion protein is synthetized and secreted into the culture supernatant (Fig. 5C, D). Notably, the prediction of *N*-glycosylation sites revealed the presence of three potential motifs in KpPguB (web reference 9) (Fig. 5B). Therefore, exporting this bacterial enzyme via the conventional secretion pathway in eukaryotes would very likely lead to artificial *N*-glycosylation, which might interfere with its activity. DNS assays using culture supernatants and polygalacturonic acid as a substrate confirmed that KpPguB was secreted and active. The amount of released reducing groups after 6 h was negligible, while after 24 h low amounts of about 0.5 mM reducing groups could be detected (Fig. 5E). This is in line with the assumption, that exo-acting enzymes show low activities on large polymeric substrates due to the low availability of polymer ends.

A similar strategy was followed to test a bacterial endo-polygalacturonase, using Peh1 from *Pectobacterium carotovorum* (PcPeh1; accession number **M83222.1**; GH28) (78). This protein even contains up to six predicted *N*-glycosylation motifs (Fig. 5B), again suggesting that unconventional secretion is a valuable tool to export the protein while avoiding potentially deleterious post-translational modifications. Also in this case, Western blot analysis and DNS assays confirmed secretion and activity with about 1 mM released reducing groups (Fig. 5C-E).

Overall, the experiments indicated that bacterial polygalacturonases could be expressed and secreted in an active state using the unique unconventional secretion system. Microscopy confirmed that the overexpression of the transgenes do not cause morphological side-effects (Fig. S3). Thus, the intrinsic repertoire can be complemented with bacterial enzymes. However, in comparison to the bacterial enzyme, the intrinsic endo-polygalacturonase did show a higher activity suggesting that the amounts of unconventionally released bacterial enzymes might need further improvements. Limiting yields of the unconventional secretion pathway have been observed earlier and are currently addressed by different optimization steps (30).

3.4 Complementation with conventionally secreted heterologous fungal polygalacturonases

Next, the performance of heterologous fungal polygalacturonases was investigated. Initially, the conventionally secreted fungal exo-polygalacturonase PgaX from *Aspergillus tubingensis* (AtPgaX; accession number CAA68128.1; GH28) was tested (79). Therefore, a published strain carrying a codon-optimized gene encoding an SHH-tagged version of AtPgaX under control of the P_{oma} in the *ip* locus of AB33P5ΔR was used (AB33P5ΔR/AtPgaX) (54). The corresponding enzyme was conventionally secreted via the endomembrane system using its native N-terminal signal peptide (Fig. 6A, B). To confirm expression and secretion of the heterologous protein, Western blot analyses of cell extracts and culture supernatants were performed (Fig. 6C, D). Specific bands were detected for AtPgaX running significantly higher than its expected size of 56.5 kDa (Fig. 6C, D) (79). The enzyme carries eight predicted *N*-glycosylation sites (Fig. 6B; web reference 9) for modification in the endomembrane system suggesting that the size shift could be due to posttranslational modifications. Indeed, deglycosylated protein was strongly reduced in size and ran approximately at the expected height (Fig. 6C, D). Enzyme activity of AB33P5ΔR/AtPgaX culture supernatant was assayed by DNS assays using polygalacturonic acid as a substrate (Fig. 6E). Compared to the control, significantly higher amounts of reducing groups were detected when testing culture supernatants obtained from the strain expressing the heterologous fungal enzyme, demonstrating that it is functionally secreted in *U. maydis*. However, only slight activity with release of about 2.5 mM reducing groups was observed (24 h incubation; Fig. 6E). This is in line with the previously observed low metabolic activity of this strain on polygalacturonic acid (54).

To evaluate the enzymatic power of heterologous fungal enzymes in comparison to intrinsic UmPgu1, a potent endo-polygalacturonase from *A. aculeatus* (AaPgu1, accession number **XM_020201835.1**; GH28) was also tested (73). The corresponding strain was

generated with a similar strategy yielding AB33P5ΔR/AaPgu1. Western blot analyses confirmed that the enzyme was produced and secreted. Consistent with the absence of *N*-glycosylation sites, it did not show a major size shift as observed for AtPgaX (Fig. 5B-D). In DNS assays up to 10 mM reducing groups were released from polygalacturonic acid (24 h incubation; Fig. 6E), confirming that the heterologous enzyme was secreted in an active state. Again, the morphology of the modified strains was not changed compared to the progenitor strain (Fig. S3), indicating that no side-effects were caused by overexpression of the transgenes.

In summary, the results suggest that the enzyme repertoire of *U. maydis* can be complemented by both bacterial and eukaryotic enzymes. Importantly, comparing the different heterologous enzymes, fungal polygalacturonases exported by conventional secretion turned out to release the highest amounts of reducing groups and are therefore likely to be the best candidates for use in polygalacturonic acid degradation. More specifically, the strong performance of AaPgu1 suggests that it should be preferred to the intrinsic endo-polygalacturonase UmPgu1 that only released up to about 6.5 mM reducing groups (dashed line, Fig. 6E). The AtPgaX producing strain could be exploited to supplement *U. maydis* cultures with the required exo-polygalacturonase activity.

Endo- and exo-polygalacturonases are supposed to act synergistically on the degradation of polygalacturonic acid to produce monomeric galacturonic acid for uptake and metabolization (80). Therefore, the next step towards efficient consolidated polygalacturonic acid utilization was to combine these enzyme activities (Fig. 7A). Therefore, the generated culture supernatants of the strains AB33P5ΔR/AtPgaX and AB33P5ΔR/AaPgu1 secreting the potent fungal polygalacturonases were mixed exemplary to conduct an enzyme assay (Fig. 7B, left bars). In addition, since up to now all enzymes in this study were overexpressed in separate strains, the potential of co-fermentation of those strains was tested. In future, this approach would allow for a flexible adaptation of strain mixtures to the respective substrate. For co-

fermentation, the two strains were inoculated in a 1:1 ratio starting at a total optical density of 0.1. DNS assays using the culture supernatant of this co-fermentation (Fig. 7B, right bars) revealed similar enzyme activity compared to the mixed culture supernatants of axenic cultures. In both experiments, about 12 mM reducing groups were released after 24 h (Fig. 7B). This suggests that both approaches yield approximately equal enzyme mixtures and that enzymes work together, yielding synergistic amounts of reducing groups compared to the individual cultivations which contain twice the amount of supernatant than the mixed supernatant assay (compare to Fig. 6E). The fact that released groups did only double with a four-fold increase of the incubation time (6 vs. 24 h) is likely due to product inhibition (54).

In summary, co-fermentations are a practical tool to analyze different combinations of hydrolytic enzymes.

3.5 Following the physiological parameters during growth on polygalacturonic acid using RAMOS

The previously used enzyme assays clearly demonstrated that *U. maydis* could be complemented by heterologous pectinolytic enzymes. However, due to product inhibition and low resolution over time, these offline *in vitro* assays only allow limiting conclusions, compared to direct cultivations on polygalacturonic acid (79). Hence, application of our established respiration activity monitoring system (RAMOS) enabled a detailed insight into the physiology of the engineered strains. This method takes advantage of the fact that sugar consumption is stoichiometrically coupled to oxygen uptake (81, 82). In a previous study, we used the AtPgaX overexpressing strain in axenic culture to develop this technique for monitoring the behavior on polygalacturonic acid (54).

In a first experiment, strain AB33P5ΔR/UmPgu1 overexpressing the intrinsic endo-polygalacturonase was grown on 20 g/L galacturonic acid or polygalacturonic acid (Fig. 8). To boost initial growth and enzyme production, all cultivations were supplemented with 4 g/L glucose as a first carbon source (Fig. 8A). Both cultures first grew on the preferred substrate

glucose, which led to a steep exponential increase of the OTR up to 11 mmol/L/h. After 7.5 h, glucose was depleted and the OTR dropped down to about 2.4 mmol/L/h. At this point, growth on the second carbon source, galacturonic acid (Fig. 8A, blue curves) or polygalacturonic acid (Fig. 8A, black curve), respectively, was initiated. As described for the progenitor strain AB33P5ΔR (54), cells of AB33P5ΔR/UmPgu1 adapted for the growth on galacturonic acid during this phase of low metabolic activity, starting after about 10 h of cultivation time. The metabolic switch can easily be detected in the course of the respiratory quotient (RQ, Fig. 8B): During consumption of glucose, RQ values of 1.1 are observed while during galacturonic acid consumption, the RQ increases to values of 1.4 (Fig. 8B, blue curves). This is in line with our previous RAMOS experiments and is attributed to the specific reduction levels of the substrates (54). In comparison to consumption of glucose, the OTR increase during growth on galacturonic acid as carbon source is less steep (Fig. 8A, blue curves), suggesting that galacturonic acid is only slowly metabolized. Microscopic imaging of the cells verified the presence of mostly living cells without excessive signs of cellular stress like abnormal morphologies or the formation of stress hyphae for both cultures during growth on both glucose and galacturonic acid (Fig. S4). The culture growing on galacturonic acid (Fig. 8A, black line and Fig. S4B) reached an OD_{600} of 8.2 at the end of cultivation.

HPLC analysis confirmed that galacturonic acid was consumed completely during the course of the experiment (data not shown). As described previously, the overall consumed oxygen during galacturonic acid metabolization can be used to estimate the residual galacturonic acid concentration (Fig. 8C, blue curves) (54). This estimation yielded a final galacturonic acid concentration of about 2 g/L (or 10% of the initial galacturonic acid concentration) at the end of cultivation deviating from the HPLC analysis. However, the deviation could be explained by different applied *U. maydis* strains and slightly different initial pH between this experiment and the underlying correlation of oxygen and galacturonic acid consumption that was published previously (54). Those differences could change

metabolic fluxes including the yield coefficient for biomass formation ($Y_{X/galacturonic\ acid}$). Thus, the stoichiometric coefficients of oxygen and galacturonic acid could differ, leading to the observed deviation between estimated and measured galacturonic acid concentration.

In contrast to the experiments on galacturonic acid, no metabolic activity could be detected for AB33P5ΔR/UmPgu1 on polygalacturonic acid (Fig. 8A, black curves). The cultivation reached OD_{600} values of about 1.4 at the end of the cultivation, being far below the final OD_{600} of 8.2 during growth on galacturonic acid. The determination of OD_{600} or cell dry weight during cultivations on polygalacturonic acid is very error prone. Polygalacturonic acid supplementation causes elevated levels of turbidity in liquid media and it sediments during centrifugation. These characteristics falsify the measurement of OD_{600} or cell dry weight, respectively. Due to the unknown fraction of hydrolyzed polygalacturonic acid during the cultivation, the OD_{600} was compared for both cultivations at the end of the cultivation. At this time point, the turbidity is caused exclusively by the cells. Microscopic analysis of the cells did not reveal any signs of enhanced cell death or abnormal morphologies even at later time points, suggesting that the culture was in a resting stage rather than dying (Fig. S4). Taken together, the measurement of metabolic activity of AB33P5ΔR/UmPgu1 during cultivation on polygalacturonic acid clearly indicates that the activity of only the activated intrinsic endo-polygalacturonase enzyme is not sufficient to permit growth on the polymer. Endo-polygalacturonases typically release oligogalacturonates with a degree of polymerization of 2 to 4, which cannot be transported across the cell membrane without further breakdown (7). Hence, although the respective enzyme activity could be detected (Fig. 4B), activation of only the intrinsic enzyme for polygalacturonic acid degradation did not enable growth on polygalacturonic acid. This confirms that complementation with further enzymes, especially exo-polygalacturonases, is needed to generate monomeric galacturonic acid.

3.6 Characterizing co-fermentations using RAMOS

Earlier experiments suggested that a combination of endo- and exo-polygalacturonase activity could be beneficial for polygalacturonic acid degradation (ref. Fig. 7B). Those supernatants were, however, generated using glucose as carbon source. To evaluate the performance of co-fermentations on polygalacturonic acid, we used strain AB33P5ΔR/AtPgaX expressing the heterologous exo-polygalacturonase from *A. terreus* (ref. Fig. 6E) and tested the effects of adding strains producing intrinsic, fungal or bacterial endo-polygalacturonase (ref. Fig. 4B, Fig. 5E and Fig. 6E, respectively) using the RAMOS technique (Fig. 9). All cultivations were conducted in biological duplicates and showed an excellent reproducibility (Fig. S5). Substrate conversion of AB33P5ΔR/AtPgaX in axenic culture was clearly limited (Fig. 9A, blue). The residual polygalacturonic acid calculated from the overall consumed oxygen during galacturonic acid consumption indicated a polygalacturonic acid consumption of < 56% after 39.5 h of cultivation time. The addition of the strain expressing intrinsic endo-polygalacturonase UmPgu1 led to an increased overall substrate consumption of 85% (Fig. 9C). The maximal OTR during galacturonic acid consumption, representing the overall enzymatic activity, was comparable to the axenic culture of the *U. maydis* strain AB33P5ΔR/AtPgaX, but the polygalacturonic acid consumption phase was elongated until > 55.5 h of cultivation time. This indicates that the addition of endo-polygalacturonase activity led to an increased substrate accessibility for the exo-polygalacturonase enzyme. The co-fermentation with the bacterial endo-polygalacturonase PcPeh1-Cts1 expressing strain showed a slightly lower maximal OTR, while the consumption phase was elongated also in comparison to the axenic culture to 60.5 h. The overall substrate consumption was comparable to the co-fermentation with the UmPgu1 expressing strain at 81%. Lower maximal OTR and elongated cultivation time indicate a low enzymatic activity for PcPeh1-Cts1, that correlates well with the offline

determined enzymatic activities for PcPeh1-Cts1 (Fig. 5E) compared to the intrinsic UmPgu1 (Fig. 4B).

Importantly, addition of the strain expressing fungal AaPgu1 did strongly increase the maximal OTR and led to the fastest consumption of polygalacturonic acid. In total, 79% of the supplemented polygalacturonic acid was consumed after only 32.5 h of cultivation time. The OTR profile mirrors precisely the growth on monomeric galacturonic acid (ref. Fig. 8A, blue; note the different time scale on the x-axis). As already discussed for the growth on monomeric galacturonic acid, the estimated residual galacturonic acid could differ for different *U. maydis* strains and cultivation conditions. Thus, in contrast to axenic cultures of AB33P5ΔR/AtPgaX on polygalacturonic acid, the substrate might have been consumed completely in all three co-fermentations after different times of cultivation. The fast growing co-fermentation of AB33P5ΔR/AtPgaX and AB33P5ΔR/AaPgu1 is a potent means to degrade the polymer polygalacturonic acid. Microscopic observations of the co-culture confirmed that the majority of cells was healthy and that it did not contain elevated amounts of cells with abnormal morphologies (Fig. S4).

The influence of three enzymatic compositions was tested by varying the inoculation ratio of the most powerful strain combination. AB33P5ΔR/AtPgaX and AB33P5ΔR/AaPgu1, overexpressing fungal endo- and exo-polygalacturonase were co-fermented with a relative inoculation ratio of 5:1; 1:1 and 1:5 while maintaining a total initial OD_{600} of 0.6 (Fig. 10). A ratio of 1:1 and 1:5 (surplus of exo-polygalacturonase, Fig. 10B and C, respectively) resulted in efficient consumption of polygalacturonic acid with complete polygalacturonic acid hydrolysis. A 5:1 ratio (surplus of endo-polygalacturonase, Fig. 10A) resulted in an elongated polygalacturonic acid consumption phase. Maximal values were reached after 20.5 h of cultivation time. From that time point on, the OTR slowly decreased over a time span of 27 h, indicating a limitation in monomeric galacturonic acid even in the presence of polygalacturonic acid. A basal OTR level of 2 mmol/L/h was reached after 47.5 h. Compared

to this cultivation, an inoculation ratio of 1:1 (Fig. 10B) and 1:5 (surplus of exo-polygalacturonase, Fig. 10C) showed maximal OTRs after 28 h. In those co-fermentations, the OTR reached a basal level of 2 mmol/L/h after 36 h. The sharp drop in the OTR over a short time span (9.5 and 8 h for a ratio of 1:1 and 1:5 (surplus of exo-polygalacturonase), respectively) indicates that both, galacturonic acid and polygalacturonic acid were depleted. At the end of the cultivation, similar OD_{600} levels (8.9 ± 0.4) were reached for all co-fermentations. This indicates that the overall consumption of polygalacturonic acid is similar with different inoculation ratios, but the time until all available polygalacturonic acid is consumed, differs. Interestingly, offline determination of galacturonic acid in these co-fermentations revealed that in all cases, the monomer accumulated during growth on glucose (until 9 h of cultivation time), which can be attributed to the expression of hydrolytically active enzyme from the very beginning of the cultivation. Interestingly, galacturonic acid accumulated further for a ratio of 1:1 (Fig. 10B, blue line) and 1:5 (surplus of exo-polygalacturonase, Fig. 10C, blue line) during the first hours of growth on galacturonic acid. This suggests that galacturonic acid uptake is a limiting step in the cultivation.

Cultivation data of the most efficient co-fermentation with an inoculation ratio of 1:5 (initial OD_{600} = 0.1 for endo-polygalacturonase strain AB33P5ΔR/AaPgu1 and OD_{600} = 0.5 for exo-polygalacturonase strain AB33P5ΔR/AtPgaX) was analyzed in more detail with respect to the galacturonic acid liberation rate (Fig. 11). Online measurement of the RQ (Fig. 11A, red lines) clearly separates the glucose and galacturonic acid consumption phases. The correlation between oxygen and galacturonic acid consumption, described in the materials and methods section 2.8, was applied to calculate the overall consumed amount of galacturonic acid over time (Fig. 11B, green lines) (54). Both fractions of galacturonic acid, offline measured concentration and calculated concentration of consumed galacturonic acid were used to determine the total liberated amount of galacturonic acid during the cultivation (Fig. 11B, black lines, see also materials and methods section 2.10). The temporal derivative of this

total liberated galacturonic acid represents the galacturonic acid liberation rate (Fig. 11C, black line). During growth on glucose, the enzyme is produced efficiently, leading to an increase of the galacturonic acid liberation rate to 1.3 g/L/h. During the galacturonic acid consumption phase, the galacturonic acid liberation rate decreases to < 0.4 g/L/h. This behavior can be explained by the development of the pH value (Fig. 11C, yellow line). During growth on glucose, the pH decreases to 4.6. The expressed exo-polygalacturonase AtPgaX has a pH optimum at 4.5 (79). This value fits very well to the cultivation pH at this time point. As the pH increases to values up to 6.7 during consumption of galacturonic acid, the enzyme activity is likely to decrease substantially, leading to a significantly decreased galacturonic acid liberation rate. Therefore, the course of the pH mirrors very well the course of the liberation rate.

4. Conclusions

In the present study, bioinformatic analyses, sophisticated strain generation and online monitoring techniques were combined to establish and follow polygalacturonic acid degradation and subsequent metabolization of its monomer galacturonic acid by *U. maydis* growing in a yeast-like morphology. This is a first and essential step towards pectin valorization. Intriguingly, bacterial enzymes were shown to be exported in an active state by unconventional secretion. However, yields are yet limiting. The recent discovery of the novel lock-type secretion pathway will help to improve the system such that this option might constitute an additional valuable tool to improve biomass degradation in the future.

The present study has also proven that co-fermentations are a promising means to combine enzyme activities without tedious generation of strains carrying multiple enzymes. This finding will be further exploited by mixing distinct master strains for efficient hydrolysis of complex substrates like pectin or sugar beet pulp. These mixtures can be evaluated with high resolution and throughput thanks to the RAMOS read-out for characterization of enzyme

production and biomass hydrolysis (54). It is generally beneficial if the cultivation shows a fast sugar uptake rate, because inhibition by products of the enzymatic hydrolysis of biomass is reduced and the released sugars are directly fermented. Hence, product inhibition does not play a major role in efficient one-pot consolidated bioprocesses (83, 84). . Therefore, the online read-out of the RAMOS technique has proven to be a reliable and practical alternative to offline sampling for the characterization of cultures growing on polygalacturonic acid. The microbial system still needs to be streamlined towards the more complex substrate pectin by insertion of additional enzymes, as well as towards higher efficiency by increasing the amount of secreted enzymes.

The present work is a solid foundation for establishing an efficient consolidated bioprocess for pectin degradation and subsequent production of glycolipids or organic acids in the future.

Funding information

The scientific activities of the Bioeconomy Science Center were financially supported by the Ministry of Culture and Science within the framework of the NRW Strategieprojekt BioSC (No. 313/323-400-002 13). The work was funded in part by grants from the Deutsche Forschungsgemeinschaft to MF, CEPLAS EXC1028.

Author contributions

P.S., M.M., S.SC. and S.ST. designed and performed the experiments. K.S., M.T., N.I., N.W., J.B., and M.F. directed the study. K.S. wrote the manuscript with input of all co-authors.

Competing interests statement

The authors have no competing interests to declare.

Acknowledgements

We thank B. Axler for excellent technical support and E. Geiser for initial assessments of growth on galacturonate. F. Finkernagel, M. Vraneš and J. Kämper provided a bioinformatics tool for automated generation of *U. maydis* dicodon-optimized sequences. We thank T. Häßler and A. Schonhoff for their support in the economic evaluation of future industrial processes.

References

1. Porro D, Branduardi P, Sauer M, Mattanovich D. Old obstacles and new horizons for microbial chemical production. Curr Current Opinion in Biotechnology. 2014;30:101-6.
2. Morais ARC, Dworakowska S, Reis A, Gouveia L, Matos CT, Bogdał D, et al. Chemical and biological-based isoprene production: Green metrics. Catal Today. 2015;239:38-43.
3. Edwards M, Doran-Peterson J. Pectin-rich biomass as feedstock for fuel ethanol production. Appl Microbiol Biotechnol. 2012;95(3):565-75.
4. De Carvalho J, Magalhaes A, Soccol C. Biobased itaconic acid market and research trends - is it really a promising chemical? Chim Oggi - Chem Today. 2018;36:56.
5. Glass NL, Schmoll M, Cate JH, Coradetti S. Plant cell wall deconstruction by ascomycete fungi. Annu Rev Microbiol. 2013;67:477-98.
6. Lampugnani ER, Khan GA, Somssich M, Persson S. Building a plant cell wall at a glance. J Cell Sci. 2018;131(2):jcs207373.
7. Jayani RS, Saxena S, Gupta R. Microbial pectinolytic enzymes: A review. Process Biochem. 2005;40(9):2931-44.
8. Caffall KH, Mohnen D. The structure, function, and biosynthesis of plant cell wall pectic polysaccharides. Carbohydr Res. 2009;344(14):1879-900.
9. Yadav S, Yadav PK, Yadav D, Yadav KDS. Pectin lyase: A review. Process Biochem. 2009;44(1):1-10.
10. Senechal F, Wattier C, Rusterucci C, Pelloux J. Homogalacturonan-modifying enzymes: structure, expression, and roles in plants. J Exp Bot. 2014;65(18):5125-60.
11. de Vries RP. Regulation of *Aspergillus* genes encoding plant cell wall polysaccharide-degrading enzymes; relevance for industrial production. Appl Microbiol Biotechnol. 2003;61(1):10-20.
12. Ohm RA, de Jong JF, Lugones LG, Aerts A, Kothe E, Stajich JE, et al. Genome sequence of the model mushroom *Schizophyllum commune*. Nat Biotechnol. 2010;28(9):957-63.
13. Blanco P, Sieiro C, Villa TG. Production of pectic enzymes in yeasts. FEMS microbiology letters. 1999;175(1):1-9.
14. Benz JP, Protzko RJ, Andrich JM, Bauer S, Dueber JE, Somerville CR. Identification and characterization of a galacturonic acid transporter from *Neurospora crassa* and its application for *Saccharomyces cerevisiae* fermentation processes. Biotechnol Biofuels. 2014;7(1):20.
15. Biz A, Sugai-Guerios MH, Kuivanen J, Maaheimo H, Krieger N, Mitchell DA, et al. The introduction of the fungal D-galacturonate pathway enables the consumption of D-galacturonic acid by *Saccharomyces cerevisiae*. Microb Cell Fact. 2016;15(1):144.
16. Glauche F, Glazyrina J, Cruz Bournazou MN, Kiesewetter G, Cuda F, Goelling D, et al. Detection of growth rate-dependent product formation in miniaturized parallel fed-batch cultivations. Eng Life Sci. 2017;17(11):1215-20.
17. Lara-Marquez A, Zavala-Paramo MG, Lopez-Romero E, Camacho HC. Biotechnological potential of pectinolytic complexes of fungi. Biotechnol Lett. 2011;33(5):859-68.
18. Klement T, Milker S, Jäger G, Grande PM, Dominguez de Maria P, Büchs J. Biomass pretreatment affects *Ustilago maydis* in producing itaconic acid. Microb Cell Fact. 2012;11:43.
19. Papagianni M, Mattey M, Kristiansen B. Citric acid production and morphology of *Aspergillus niger* as functions of the mixing intensity in a stirred tank and a tubular loop bioreactor. Biochem Eng J. 1998;2(3):197-205.

20. Geiser E, Reindl M, Blank LM, Feldbrügge M, Wierckx N, Schipper K. Activating intrinsic carbohydrate-active enzymes of the smut fungus *Ustilago maydis* for the degradation of plant cell wall components. Appl Environ Microbiol. 2016;82(17):5174-85.
21. Feldbrügge M, Kellner R, Schipper K. The biotechnological use and potential of plant pathogenic smut fungi. Appl Microbiol Biotechnol. 2013;97(8):3253-65.
22. Vollmeister E, Schipper K, Baumann S, Haag C, Pohlmann T, Stock J, et al. Fungal development of the plant pathogen *Ustilago maydis*. FEMS Microbiol Rev. 2012;36(1):59-77.
23. Djamei A, Kahmann R. *Ustilago maydis*: dissecting the molecular interface between pathogen and plant. PLoS Pathog. 2012;8(11):e1002955.
24. Brachmann A, König J, Julius C, Feldbrügge M. A reverse genetic approach for generating gene replacement mutants in *Ustilago maydis*. Molecular genetics and genomics : MGG. 2004;272(2):216-26.
25. Terfrüchte M, Joehnk B, Fajardo-Somera R, Braus GH, Riquelme M, Schipper K, et al. Establishing a versatile Golden Gate cloning system for genetic engineering in fungi. Fungal Genet Biol. 2014;62:1-10.
26. Schuster M, Schweizer G, Reissmann S, Kahmann R. Genome editing in *Ustilago maydis* using the CRISPR-Cas system. Fungal Genet Biol. 2016;89:3-9.
27. Khrunyk Y, Münch K, Schipper K, Lupas AN, Kahmann R. The use of FLP-mediated recombination for the functional analysis of an effector gene family in the biotrophic smut fungus *Ustilago maydis*. New Phytol. 2010;187(4):957-68.
28. Stock J, Sarkari P, Kreibich S, Brefort T, Feldbrügge M, Schipper K. Applying unconventional secretion of the endochitinase Cts1 to export heterologous proteins in *Ustilago maydis*. J Biotechnol. 2012;161(2):80-91.
29. Carstensen F, Klement T, Büchs J, Melin T, Wessling M. Continuous production and recovery of itaconic acid in a membrane bioreactor. Bioresour Technol. 2013;137:179-87.
30. Terfrüchte M, Wewetzer S, Sarkari P, Stollewerk D, Franz-Wachtel M, Macek B, et al. Tackling destructive proteolysis of unconventionally secreted heterologous proteins in *Ustilago maydis*. J Biotechnol. 2018;284:37-51.
31. Brefort T, Doehlemann G, Mendoza-Mendoza A, Reissmann S, Djamei A, Kahmann R. *Ustilago maydis* as a pathogen. Annu Rev Phytopathol. 2009;47:423-45.
32. Kahmann R, Romeis T, Bölker M, Kämper J. Control of mating and development in *Ustilago maydis*. Curr Opin Genet Dev. 1995;5(5):559-64.
33. Klose J, De Sá MM, Kronstad JW. Lipid-induced filamentous growth in *Ustilago maydis*. Mol Microbiol. 2004;52(3):823-35.
34. Kahmann R, Kämper J. *Ustilago maydis*: how its biology relates to pathogenic development. New Phytologist. 2004;164(1):31-42.
35. Hosseinpour Tehrani H, Tharmasothirajan A, Track E, Blank LM, Wierckx N. Engineering the morphology and metabolism of pH tolerant *Ustilago cynodontis* for efficient itaconic acid production. Metab Eng. 2019;54:293-300.
36. Valverde ME, Paredes- López O, Pataky JK, Guevara- Lara F, Pineda TS. Huitlacoche (*Ustilago maydis*) as a food source — biology, composition, and production. Crit Rev Food Sci Nutr. 1995;35(3):191-229.
37. Bölker M, Basse CW, Schirawski J. *Ustilago maydis* secondary metabolism—From genomics to biochemistry. Fungal Genetics and Biology. 2008;45, Supplement 1:S88-S93.
38. Geiser E, Wiebach V, Wierckx N, Blank LM. Prospecting the biodiversity of the fungal family Ustilaginaceae for the production of value-added chemicals. Fungal Biology and Biotechnology. 2014;1(1):1-10.
39. Khachatryan V, Sirunyan AM, Tumasyan A, Adam W, Bergauer T, Dragicevic M, et al. Precise determination of the mass of the Higgs boson and tests of compatibility of its couplings with the standard model predictions using proton collisions at 7 and 8[Formula: see text]. Eur Phys J C Part Fields. 2015;75(5):212.

40. Regestein L, Klement T, Grande P, Kreyenschulte D, Heyman B, Massmann T, et al. From beech wood to itaconic acid: case study on biorefinery process integration. Biotechnol Biofuels. 2018;11:279.
41. Geiser E, Przybilla SK, Engel M, Kleineberg W, Büttner L, Sarikaya E, et al. Genetic and biochemical insights into the itaconate pathway of *Ustilago maydis* enable enhanced production. Metab Eng. 2016;38:427-35.
42. Doehlemann G, Wahl R, Vranes M, de Vries RP, Kämper J, Kahmann R. Establishment of compatibility in the *Ustilago maydis*/maize pathosystem. J Plant Physiol. 2008;165(1):29-40.
43. Mueller O, Kahmann R, Aguilar G, Trejo-Aguilar B, Wu A, de Vries RP. The secretome of the maize pathogen *Ustilago maydis*. Fungal Genet Biol. 2008;45 Suppl 1:S63-70.
44. Couturier M, Navarro D, Olive C, Chevret D, Haon M, Favel A, et al. Post-genomic analyses of fungal lignocellulosic biomass degradation reveal the unexpected potential of the plant pathogen *Ustilago maydis*. BMC Genom. 2012;13:57.
45. Cano-Canchola C, Acevedo L, Ponce-Noyola P, Flores-Martinez A, Flores-Carreon A, Leal-Morales CA. Induction of lytic enzymes by the interaction of *Ustilago maydis* with *Zea mays* tissues. Fungal Genet Biol. 2000;29(3):145-51.
46. Geiser E, Wierckx N, Zimmermann M, Blank LM. Identification of an endo-1,4-beta-xylanase of *Ustilago maydis*. BMC Biotechnol. 2013;13:59.
47. Hartmann HA, Krüger J, Lottspeich F, Kahmann R. Environmental signals controlling sexual development of the corn smut fungus *Ustilago maydis* through the transcriptional regulator Prf1. Plant Cell. 1999;11(7):1293-306.
48. Dimou E, Nickel W. Unconventional mechanisms of eukaryotic protein secretion. Curr Biol. 2018;28(8):R406-R10.
49. Reindl M, Hänsch S, Weidtkamp-Peters S, Schipper K. A potential lock-type mechanism for unconventional secretion in fungi. Int J Mol Sci. 2019;20(3):460.
50. Koepke J, Kaffarnik F, Haag C, Zarnack K, Luscombe NM, König J, et al. The RNA-binding protein Rrm4 is essential for efficient secretion of endochitinase Cts1. Mol Cell Proteomics. 2011;10(12):M111 011213.
51. Aschenbroich J, Hussnaetter KP, Stoffels P, Langner T, Zander S, Sandrock B, et al. The germinal centre kinase Don3 is crucial for unconventional secretion of chitinase Cts1 in *Ustilago maydis*. Biochim Biophys Acta Proteins Proteom. 2018.
52. Sarkari P, Reindl M, Stock J, Müller O, Kahmann R, Feldbrügge M, et al. Improved expression of single-chain antibodies in *Ustilago maydis*. J Biotechnol. 2014;191:165-75.
53. Terfrüchte M, Reindl M, Jankowski S, Sarkari P, Feldbrügge M, Schipper K. Applying unconventional secretion in *Ustilago maydis* for the export of functional nanobodies. Int J Mol Sci. 2017;18(5).
54. Müller MJ, Stachurski S, Stoffels P, Schipper K, Feldbrügge M, Büchs J. Online evaluation of the metabolic activity of *Ustilago maydis* on (poly)galacturonic acid. J Biol Eng. 2018;12:34.
55. Green MR, Sambrook J. Molecular cloning: A laboratory manual. Fourth edition. Cold Spring Harbor Laboratory Press. 2012:2028.
56. Kämper J, Kahmann R, Bölker M, Ma LJ, Brefort T, Saville BJ, et al. Insights from the genome of the biotrophic fungal plant pathogen *Ustilago maydis*. Nature. 2006;444(7115):97-101.
57. Haag C, Klein T, Feldbrügge M. Functional *in vivo* analysis of ESCRT components using model fungi. Methods in Mol Biol In: The ESCRT Complex: Methods and Protocols, eds Emmanuel Culetto and Renaud Legouis, Springer Science & Buisness Media New York. in press.

58. Zhou L, Obhof T, Schneider K, Feldbrügge M, Nienhaus GU, Kämper J. Cytoplasmic transport machinery of the SPF27 homologue Num1 in *Ustilago maydis*. Sci Rep. 2018;8(1):3611.
59. Nielsen H. Predicting secretory proteins with SignalP. Methods in molecular biology. 2017;1611:59-73.
60. Bosch K, Frantzeskakis L, Vranes M, Kämper J, Schipper K, Gohre V. Genetic manipulation of the plant pathogen *Ustilago maydis* to study fungal biology and plant microbe interactions. J Vis Exp. 2016(115):e54522.
61. Loubradou G, Brachmann A, Feldbrügge M, Kahmann R. A homologue of the transcriptional repressor Ssn6p antagonizes cAMP signalling in *Ustilago maydis*. Mol Microbiol. 2001;40(3):719-30.
62. Brachmann A, Weinzierl G, Kämper J, Kahmann R. Identification of genes in the bW/bE regulatory cascade in *Ustilago maydis*. Mol Microbiol. 2001;42(4):1047-63.
63. Holliday R. *Ustilago maydis*. In: King RC, editor. Bacteria, Bacteriophages, and Fungi: Springer US; 1974. p. 575-95.
64. Sievers F, Wilm A, Dineen D, Gibson TJ, Karplus K, Li W, et al. Fast, scalable generation of high-quality protein multiple sequence alignments using Clustal Omega. Mol Syst Biol. 2011;7:539.
65. Robert X, Gouet P. Deciphering key features in protein structures with the new ENDscript server. Nucleic Acids Res. 2014;42(Web Server issue):W320-4.
66. Stock J, Terfrüchte M, Schipper K. A reporter system to study unconventional secretion of proteins avoiding *N*-glycosylation in *Ustilago maydis*. In: Pompa A, De Marchis F, editors. Unconventional Protein Secretion: Methods and Protocols. New York, NY: Springer New York; 2016. p. 149-60.
67. Laemmli UK. Cleavage of structural proteins during the assembly of the head of bacteriophage T4. Nature. 1970;227(5259):680-5.
68. Miller GL. Dinitrosalicylic acid reagent for determination of reducing sugar. Anal Chem. 1959;31(3):426-8.
69. Anderlei T, Büchs J. Device for sterile online measurement of the oxygen transfer rate in shaking flasks. Biochem Eng J. 2001;7(2):157-62.
70. Anderlei T, Zang W, Papaspyrou M, Büchs J. Online respiration activity measurement (OTR, CTR, RQ) in shake flasks. Biochem Eng J. 2004;17(3):187-94.
71. CAZypedia Consortium. Ten years of CAZypedia: a living encyclopedia of carbohydrate-active enzymes. Glycobiology. 2018;28(1):3-8.
72. Federici L, Caprari C, Mattei B, Savino C, Di Matteo A, De Lorenzo G, et al. Structural requirements of endopolygalacturonase for the interaction with PGIP (polygalacturonase-inhibiting protein). Proc Natl Acad Sci USA. 2001;98(23):13425-30.
73. Abdulrachman D, Thongkred P, Kocharin K, Nakpathom M, Somboon B, Narumol N, et al. Heterologous expression of *Aspergillus aculeatus* endo-polygalacturonase in *Pichia pastoris* by high cell density fermentation and its application in textile scouring. BMC Biotechnol. 2017;17(1):15.
74. Martens-Uzunova ES, Schaap PJ. Assessment of the pectin degrading enzyme network of *Aspergillus niger* by functional genomics. Fungal Genet Biol. 2009;46 Suppl 1:S170-S9.
75. Martens-Uzunova ES, Schaap PJ. An evolutionary conserved d-galacturonic acid metabolic pathway operates across filamentous fungi capable of pectin degradation. Fungal Genet Biol. 2008;45(11):1449-57.
76. Niu J, Alazi E, Reid ID, Arentshorst M, Punt PJ, Visser J, et al. An evolutionarily conserved transcriptional activator-repressor module controls expression of genes for D-galacturonic acid utilization in *Aspergillus niger*. Genetics. 2017;205(1):169-83.

77. Ibrahim E, Jones KD, Taylor KE, Hosseney EN, Mills PL, Escudero JM. Molecular and biochemical characterization of recombinant cel12B, cel8C, and peh28 overexpressed in *Escherichia coli* and their potential in biofuel production. Biotechnol Biofuels. 2017;10:52.
78. Yuan P, Meng K, Wang Y, Luo H, Shi P, Huang H, et al. A protease-resistant exo-polygalacturonase from *Klebsiella sp*. Y1 with good activity and stability over a wide pH range in the digestive tract. Bioresour Technol. 2012;123:171-6.
79. Kester HC, Kusters-van Someren MA, Müller Y, Visser J. Primary structure and characterization of an exopolygalacturonase from *Aspergillus tubingensis*. Eur J Biochem. 1996;240(3):738-46.
80. van den Brink J, de Vries RP. Fungal enzyme sets for plant polysaccharide degradation. Appl Microbiol Biotechnol. 2011;91(6):1477.
81. Antonov E, Wirth S, Gerlach T, Schlembach I, Rosenbaum MA, Regestein L, et al. Efficient evaluation of cellulose digestibility by *Trichoderma reesei* Rut-C30 cultures in online monitored shake flasks. Microb Cell Fact. 2016;15(1):164.
82. Antonov E, Schlembach I, Regestein L, Rosenbaum MA, Büchs J. Process relevant screening of cellulolytic organisms for consolidated bioprocessing. Biotechnol Biofuels. 2017;10:106.
83. Carere RC, Sparling R, Cicek N, Levin BD. Third generation biofuels via direct cellulose fermentation. Int J Mol Sci. 2008;9(7).
84. Brunecky R, Chung D, Sarai NS, Hengge N, Russell JF, Young J, et al. High activity CAZyme cassette for improving biomass degradation in thermophiles. Biotechnol Biofuels. 2018;11(1):22.
85. Kent LM, Loo TS, Melton LD, Mercadante D, Williams MA, Jameson GB. Structure and properties of a non-processive, salt-requiring, and acidophilic pectin methylesterase from *Aspergillus niger* provide insights into the key determinants of processivity control. J Biol Chem. 2016;291(3):1289-306.

Web references

1. http://www.feedimpex.com/usage-sugar-beet-pellets; last accessed 2019/06/21
2. https://www.nordzucker.com/fileadmin/downloads/Geschaeftspartner/futtermittel_melasse/Final_Flyer_Pressschnitzel_Druck.pdf; last accessed 2019/10/09
3. http://www.cazypedia.org; last accessed 2019/06/21
4. https://fungi.ensembl.org/Ustilago_maydis/Info/Index , last accessed 2019/07/25
5. http://www.cbs.dtu.dk/services/SignalP/, last accessed 2019/06/21
6. https://blast.ncbi.nlm.nih.gov/Blast.cgi?PAGE=Proteins&PROGRAM=blastp&BLAST_PROGRAMS=blastp&PAGETYPE=BlastSearch&DATABASE=refseq_protein&DESCRIPTIONS=100; last accessed 2019/06/21
7. http://www.cbs.dtu.dk/services/SignalP-4.1/; last accessed 2019/07/25
8. https://www.ebi.ac.uk/Tools/msa/clustalo/, last accessed 2019/06/21
9. http://www.cbs.dtu.dk/services/NetNGlyc/, last accessed 2019/06/21

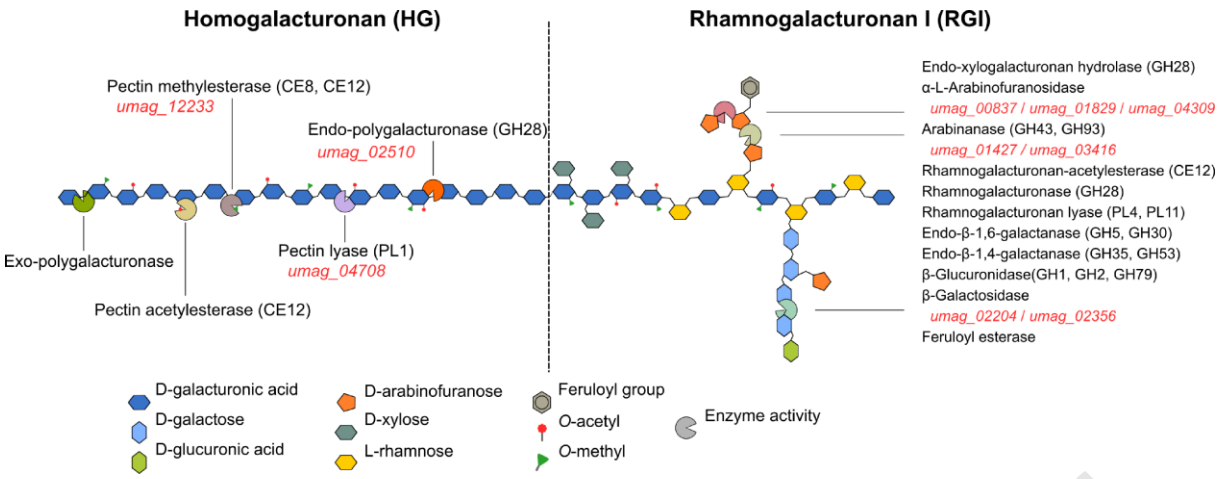

Fig. 1. Schematic structure of the most abundant pectin classes HG and RGI and relevant enzymes for degradation. Enzymes required for degradation of the two major pectin classes and their sites of action are depicted. Corresponding enzymatic domains according to CAZy database are provided in brackets. GH, glycoside hydrolase domain; PL, polysaccharide lyase domain; CE, carbohydrate esterase domain (web reference 3). The *U. maydis* genome encodes some putative pectinolytic enzymes (corresponding *umag* identifiers indicated in red; web reference 4), especially for decomposition of the polygalacturonic acid backbone in HG and the arabinose side-chains of RGI. Nevertheless, crucial enzymes for complete pectin hydrolysis are lacking. Figure adapted from Glass *et al.*, 2013 (2).

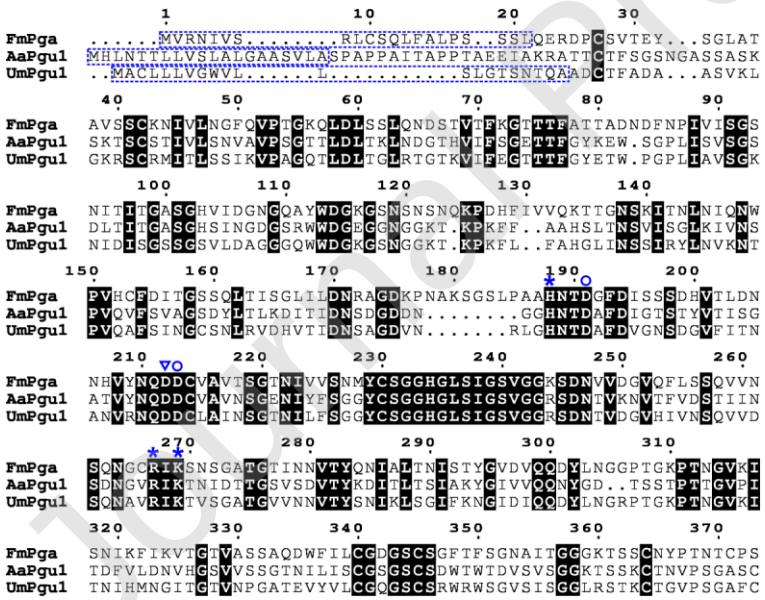

Fig. 2. Conservation of a putative endo-polygalacturonase of *U. maydis*. Amino acid alignment showing the conservation of important functional residues between the well-characterized *Fusarium moniliforme* Pga (FmPga; accession number **Q07181.1**), *Aspergillus aculeatus* Pgu1 (AaPgu1; accession number **O74213.1**) and the putative endo-polygalacturonase Pgu1 present in *U. maydis* (UmPgu1; accession number **KIS69158.1**). Blue asterisks depict residues involved in substrate binding; the blue triangle marks the aspartate residue that presumably donates protons to the glycosidic oxygen and the circles

mark residues involved in activating H_2O for the nucleophilic attack (72). The predicted N-terminal signal peptides for conventional secretion are indicated by the blue dashed boxes. Identical amino acids are depicted with a black background.

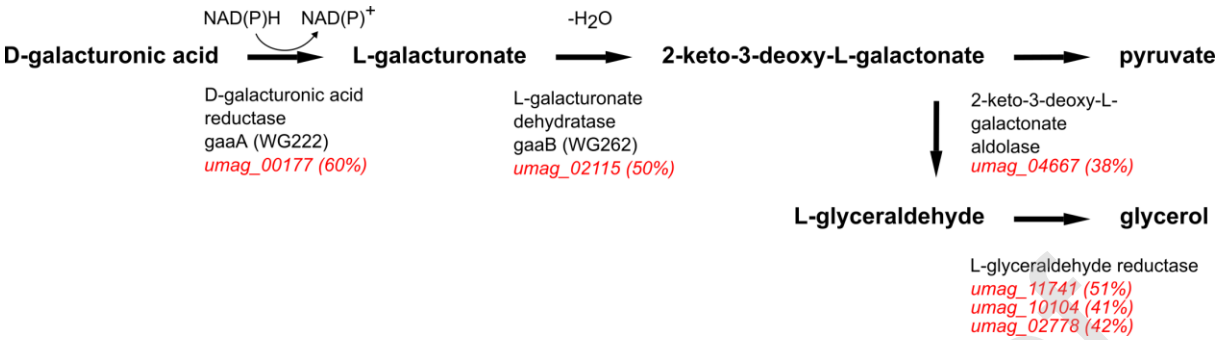

Fig. 3. Conservation of the galacturonic acid catabolic pathway between *A. niger* (75) and *U. maydis*. Numbers indicate the percentage of overall amino acid conservation. *umag* numbers (red font) correspond to respective gene identifiers found on EnsemblFungi *Ustilago maydis* genome database or NCBI. *A. niger* pathway adapted from Martens-Uzunova *et al.*, 2008 (75).

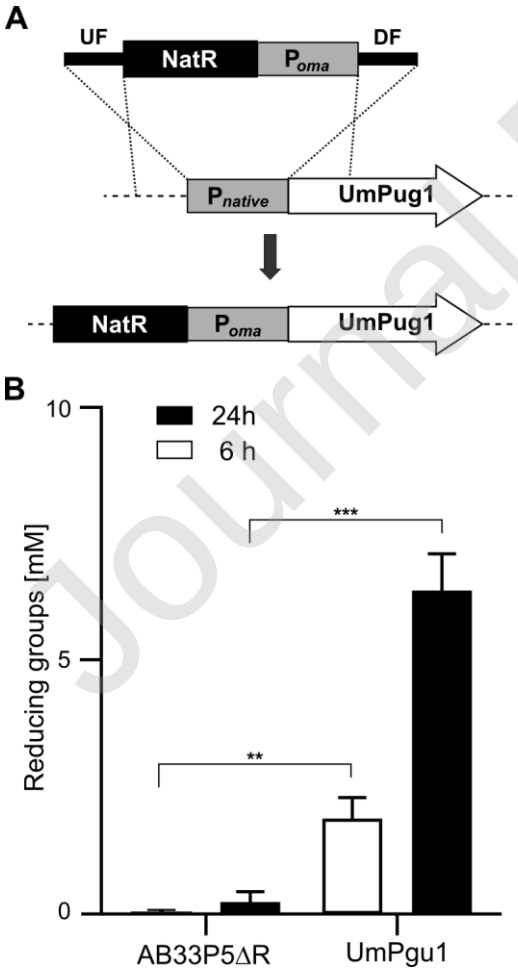

Fig. 4. Activation of an intrinsic endo-polygalacturonase. A, Schematic representation of the applied gene-activation strategy (20). The native promoter of the corresponding gene *umpgu1* (*umag_02510*) was replaced by the strong constitutive promoter P_{oma}. A nourseothricin resistance cassette (NatR) was inserted for selection. **B**, DNS assay depicting enzymatic activity of constitutively expressed intrinsic endo-polygalacturonase on polygalacturonic acid. The progenitor strain AB33P5ΔR served as control, exhibiting no significant activity. Upon incubation with polygalacturonic acid, the activated strain AB33P5Δ/UmPgu1 showed a strongly enhanced release of reducing groups. The graph represents the results of three biological replicates. Error bars depict standard deviation. **, p value < 0.01; ***, p value 0.001 (two sample *t*-test).

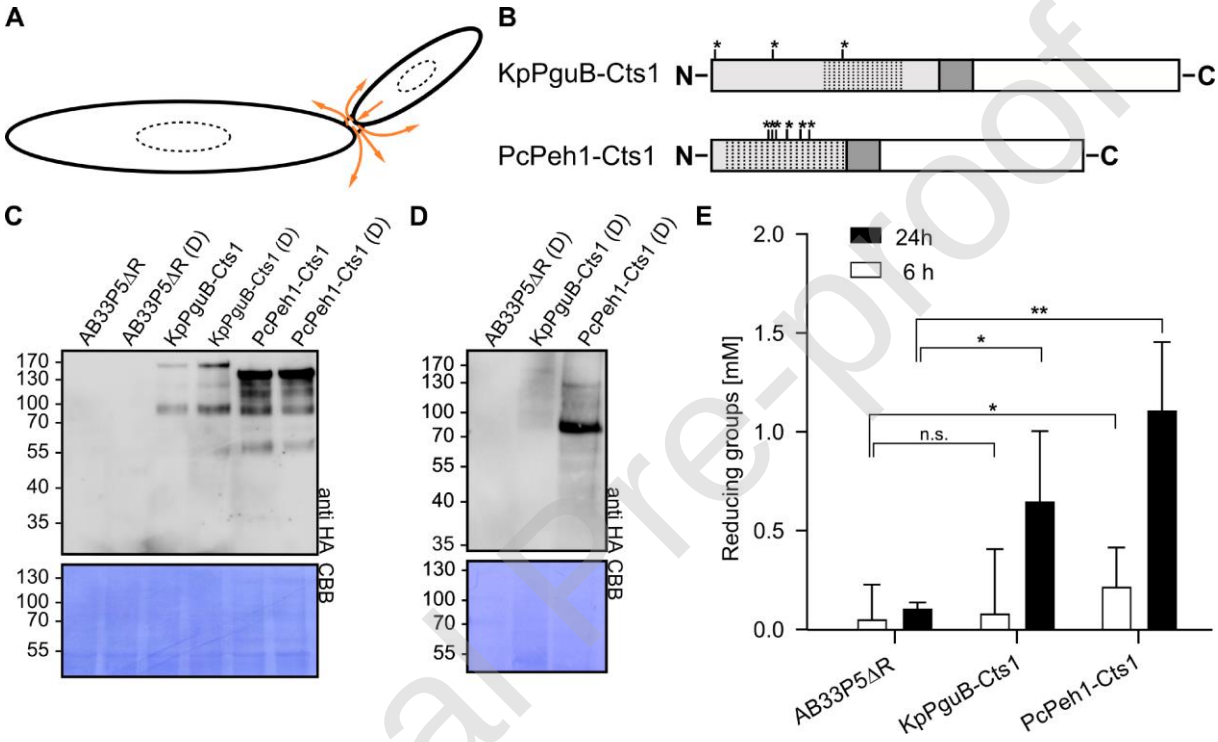

Fig. 5. Complementation with bacterial endo- and exo-polygalacturonases. A, Heterologous enzymes are secreted by lock-type unconventional secretion via the fragmentation zone of dividing yeast-like growing cells (scheme). **B**, Representation of the two bacterial Cts1-fusion proteins used for complementation. Predicted *N*-glycosylation sites of endo-polygalacturonase *P. carotovorum* Peh1 (PcPeh1, 3 predicted sites) and exo-polygalacturonase *K. pneumoniae* PguB (KpPguB, 6 predicted sites) are indicated by asterisks. Predicted N-terminal signal peptides were removed from the sequences to allow for Cts1-mediated unconventional secretion. Cts1 is indicated in white. An SHH-tag connects the two protein moieties (shown in grey). The predicted functional GH28 domains are indicated by dotted areas. **C**, Expression of bacterial polygalacturonases in AB33P5ΔR (progenitor). The Western blot analysis depicts cell extracts (10 µg), which were partially deglycosylated (D). Heterologous proteins were detected using antibodies directed against the internal HA-tag. CBB, Coomassie Brilliant Blue staining of the membrane. Expected sizes of tagged proteins: KpPguB-Cts1, 134.9 kDa; PcPeh1-Cts1, 105.1 kDa. **D**, Unconventional secretion of bacterial polygalacturonases in AB33P5ΔR as Cts1-fusion proteins. The Western blot analysis depicts precipitated and deglycosylated culture supernatants (corresponding to 20 ml culture). Proteins were detected using antibodies directed against the internal HA-tag. CBB,

Coomassie Brilliant Blue staining of the membrane. **E**, DNS assay to detect activity of heterologous enzymes from bacterial sources. In contrast to the progenitor strain AB33P5ΔR, both engineered strains release reducing groups from polygalacturonic acid. The graph represents the results of three biological replicates. Error bars depict standard deviation, n.s., p value > 0.05; *, p value < 0.05; **, p value < 0.01.

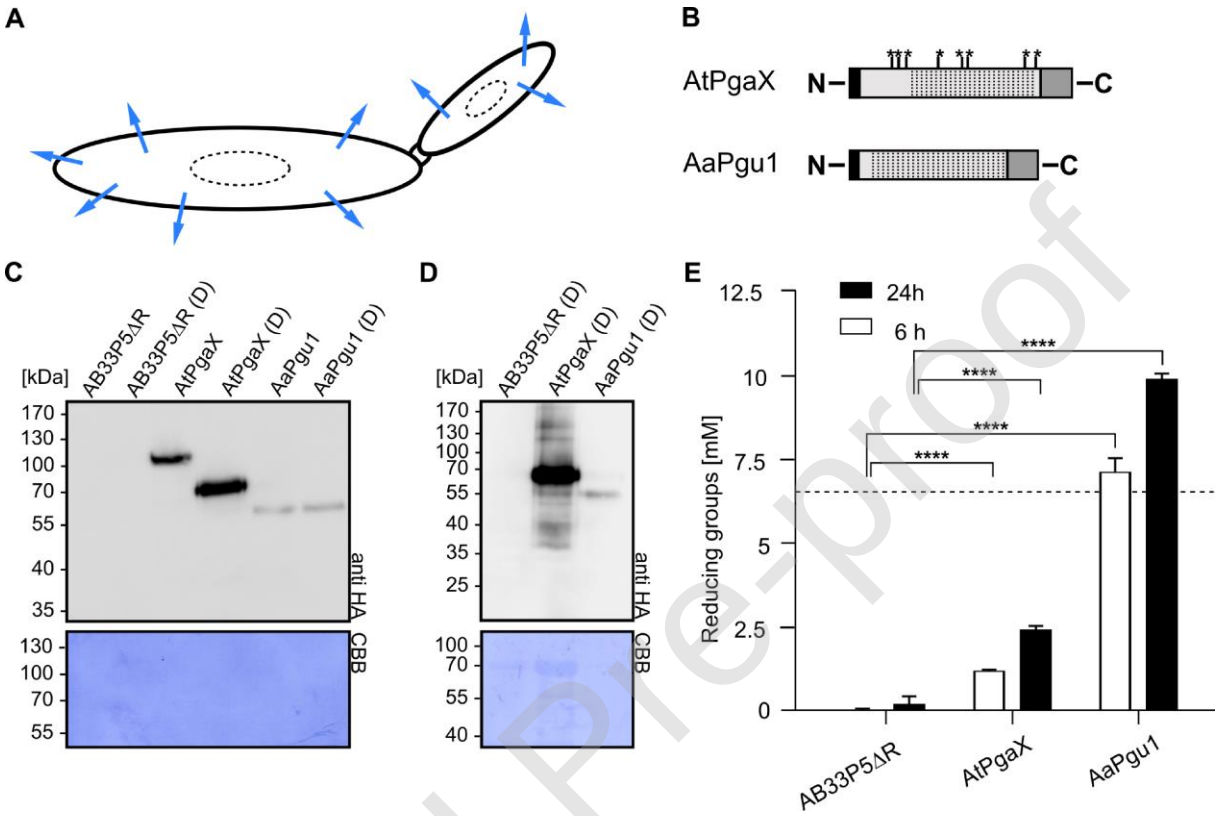

Fig. 6. Complementation with fungal endo- and exo-polygalacturonases. A, Heterologous enzymes are secreted by conventional secretion via the endomembrane system of yeast-like growing cells (scheme). **B**, Representation of the two fungal proteins used for complementation. Predicted *N*-glycosylation sites of *A. tubingensis* PgaX (AtPgaX, 8 predicted sites) and *A. aculeatus* Pgu1 (AaPgu1, 0 predicted sites) are depicted by asterisks. Predicted N-terminal signal peptides are indicated in black. The C-terminal SHH-tag is shown in grey. The predicted functional GH28 domains are indicated by dotted areas. **C**, Expression of fungal polygalacturonases in AB33P5ΔR (progenitor strain). The Western blot analysis depicts cell extracts (10 µg), which were partially deglycosylated (D). Heterologous proteins were detected using antibodies directed against the HA-tag. CBB, Coomassie Brilliant Blue staining of the membrane. Expected sizes of tagged proteins: AtPgaX, 56.5 kDa; AaPgu1, 47.1 kDa. **D**, Conventional secretion of fungal polygalacturonases in AB33P5ΔR. The Western blot analysis depicts precipitated and deglycosylated culture supernatants (corresponding to 1 ml culture). Proteins were detected using antibodies directed against the HA-tag. **E**, DNS assay to detect activity of heterologous enzymes from fungal sources on polygalacturonic acid. In contrast to the progenitor strain AB33P5ΔR, both engineered strains were active on this polymer (release of reducing groups). The amount of reducing groups liberated by the fungal endo-polygalacturonase AaPgu1 was higher compared to the intrinsic UmPgu1 (dashed line after 24 h). The graph represents the results of three biological replicates. Error bars depict standard deviation; ****, p value > 0.0001.

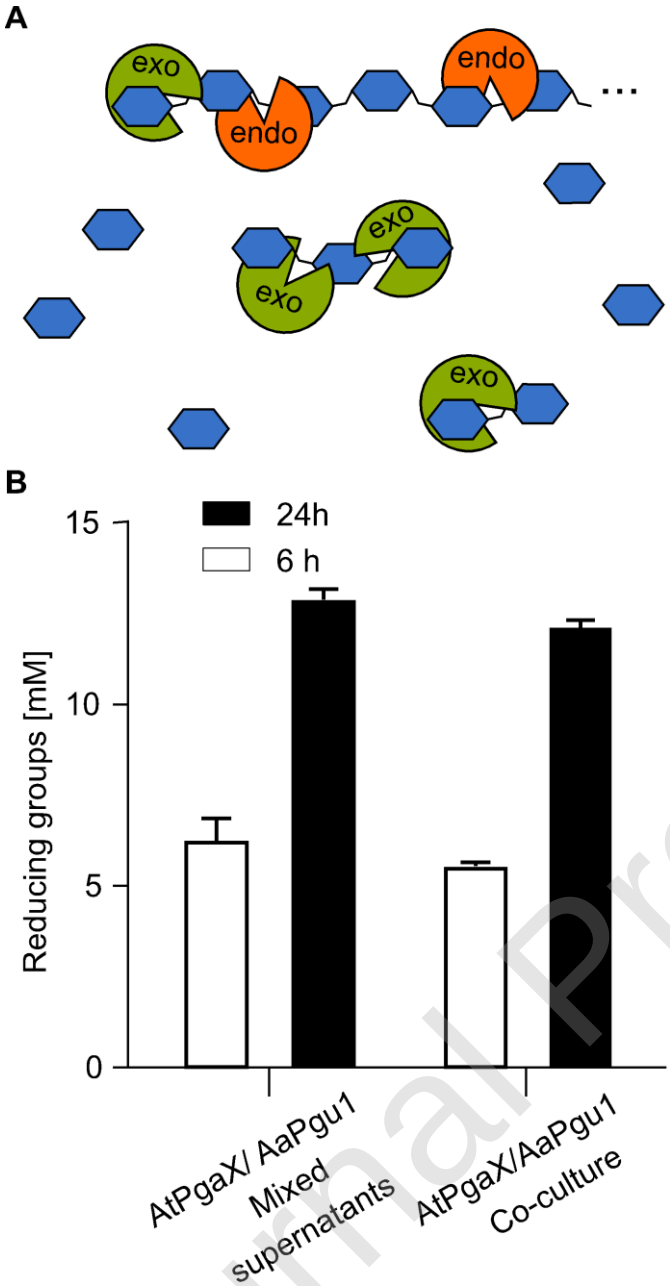

Fig. 7. Co-fermentations of fungal endo- and exo-polygalacturonases. A, Schematical representation of exo-polygalaturonases (green) and endo-polygalacturonases (orange) acting on polygalacturonic acid. **B,** Comparative DNS assays using mixed supernatants and mixed cultures of strains secreting intrinsic fungal endo- and heterologous exo-polygalacturonase. Strains AB33P5ΔR/AtPgaX and AB33P5ΔR/AaPgu1 were used for the assay. The graph represents the results of three biological replicates. Error bars depict standard deviation.

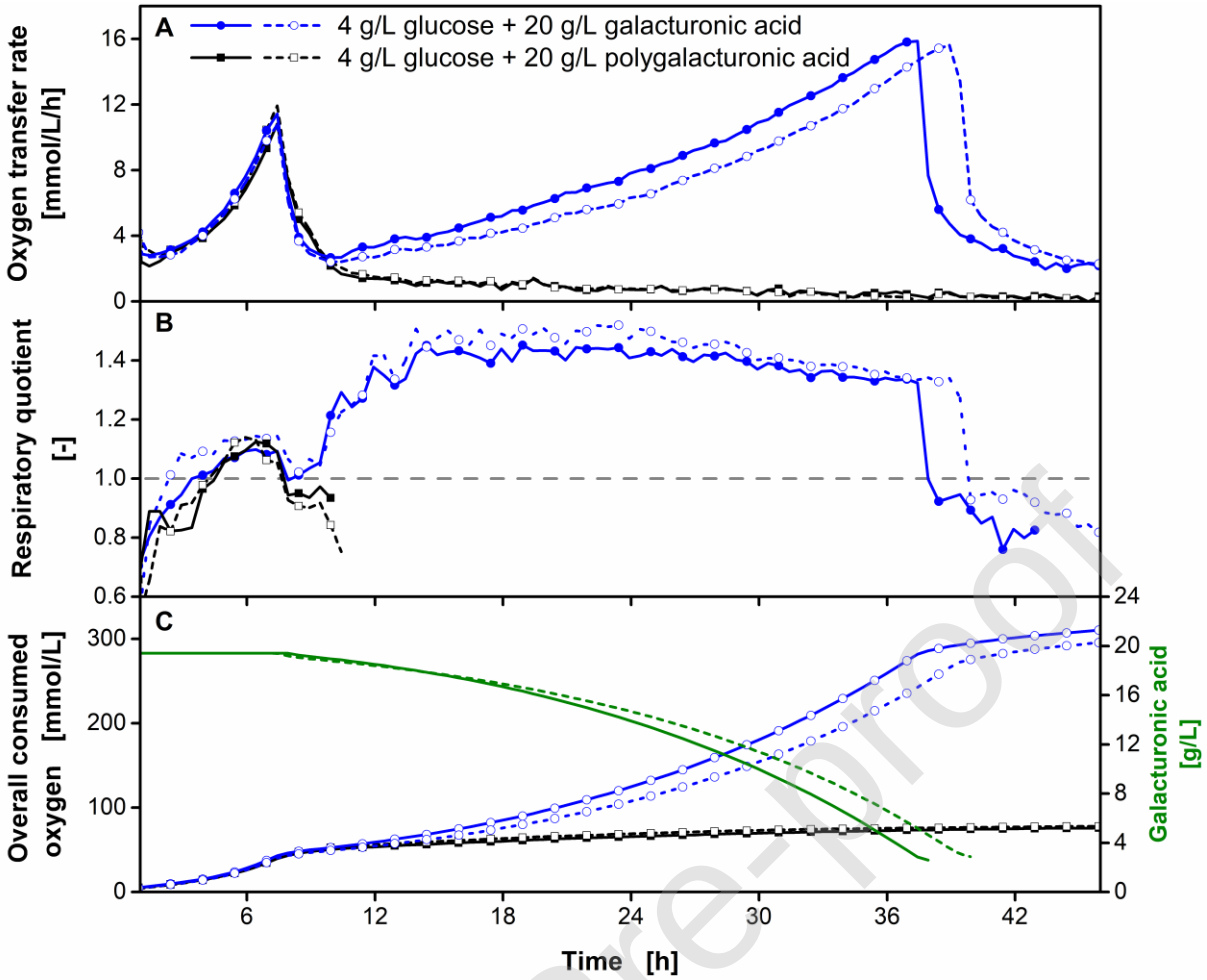

Fig. 8. Cultivation of the UmPgu1 (endo-polygalacturonase) overexpression strain on galacturonic acid and polygalacturonic acid. Strain AB33P5ΔR/UmPgu1 was grown on a mixture of glucose (Glc, 4 g/L) and (poly)galacturonic acid (20 g/L, purity 85%) as carbon sources. **A**, Biological duplicates of oxygen transfer rate, represented each as line and dashed line. **B**, Biological duplicates of respiratory quotient, represented each as line and dashed line. **C**, Biological duplicates of the overall consumed oxygen, represented each as line and dashed line. For the cultivation on galacturonic acid, the estimated residual galacturonic acid concentration (54) is shown in green. For clarity reasons, only every third data point is shown and the RQ is only shown for OTR > 2 mmol/L/h. Culture conditions: modified Verduyn mineral medium, 0.2 M MOPS, initial pH 6.0, 250 mL flask, filling volume 20 mL, shaking frequency 300 rpm, shaking diameter 50 mm, initial OD_{600} = 0.6, T = 30°C.

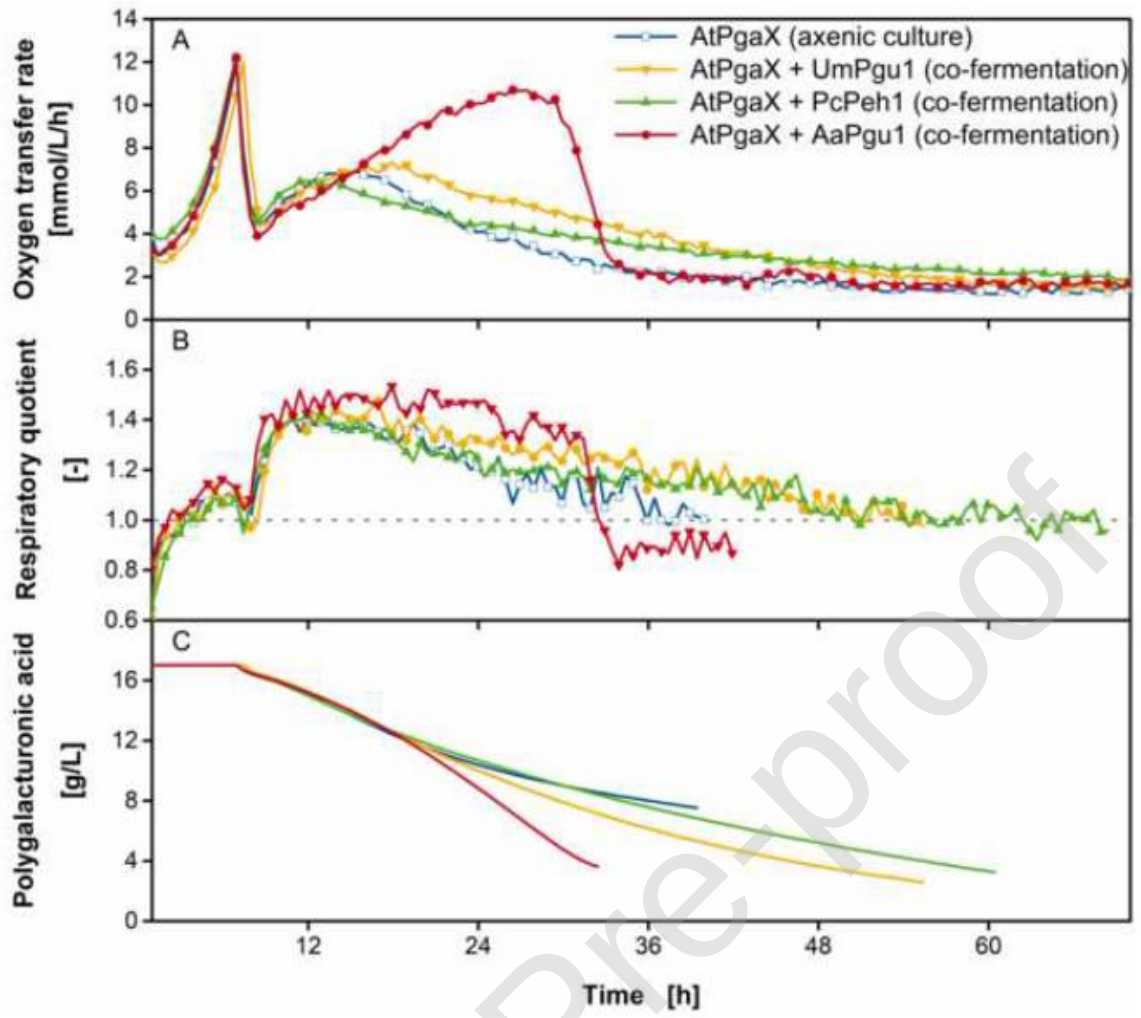

Fig. 9. RAMOS cultivation of axenic cultures and co-fermentations on polygalacturonic acid. The strains expressing AtPgaX (fungal exo-polygalacturonase), UmPgu1 (intrinsic endo-polygalacturonase), PcPeh1 (bacterial endo-polygalacturonase) and AaPgu1(fungal endo-polygalacturonase) were grown on a mixture of glucose (4 g/L) and polygalacturonic acid (20 g/L, purity 85%) as carbon sources. A, Oxygen transfer rate. B, Respiratory quotient. C, Residual substrate calculated from the overall consumed oxygen (54). End of polygalacturonic acid consumption was defined by the RQ drop below 1. For clarity reasons, only every third data point is shown and the RQ is only shown for OTR > 2 mmol/L/h. All plots represent the mean of biological duplicates (see **Error! Reference source not found.** for individual cultivations). Culture conditions: modified Verduyn mineral medium, 0.2 M MOPS, initial pH 6.0, 250 mL flask, filling volume 20 mL, shaking frequency 300 rpm, shaking diameter 50 mm, initial OD_{600} = 0.6 (inoculation ratio 1:1 for co-fermentations), T = 30 °C.

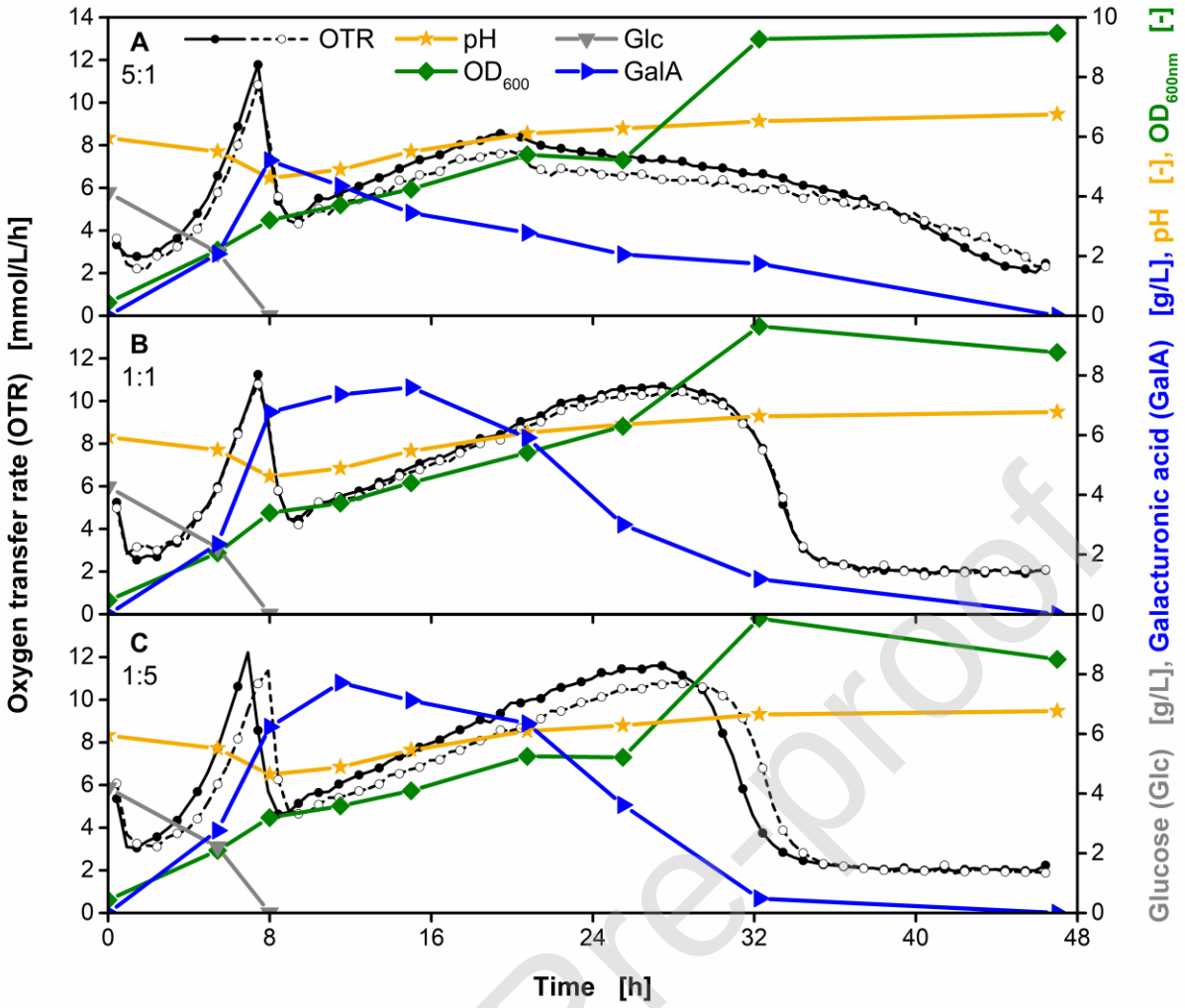

Fig. 10. Co-fermentation of AtPgaX (fungal exo-polygalacturonase) and AaPgu1 (fungal endo-polygalacturonase) overexpression strains with different inoculation ratios on polygalacturonic acid. The strain combination AB33P5ΔR/AtPgaX and AB33P5ΔR/AaPgu1 was grown in medium containing a mixture of glucose (4 g/L) and polygalacturonic acid (20 g/L, purity 85%) as carbon sources. **A**, Inoculation ratio 5:1 (OD_{600} = 0.5 for AB33P5ΔR/AaPgu1 and OD_{600} = 0.1 for AB33P5ΔR/AtPgaX). **B**, Inoculation ratio 1:1 (OD_{600} = 0.3 for both, AB33P5ΔR/AtPgaX and AB33P5ΔR/AaPgu1). **C**, Inoculation ratio 1:5 (OD_{600} = 0.1 for AB33P5ΔR/AaPgu1 and OD_{600} = 0.5 for AB33P5ΔR/AtPgaX). Continuous and dashed black lines represent biological duplicates of RAMOS cultivations. For clarity reasons, only every third data point is shown. Culture conditions: modified Verduyn mineral medium, 0.2 M MOPS, initial pH 6.0, 250 mL flask, filling volume 20 mL, shaking frequency 300 rpm, shaking diameter 50 mm, T = 30°C.

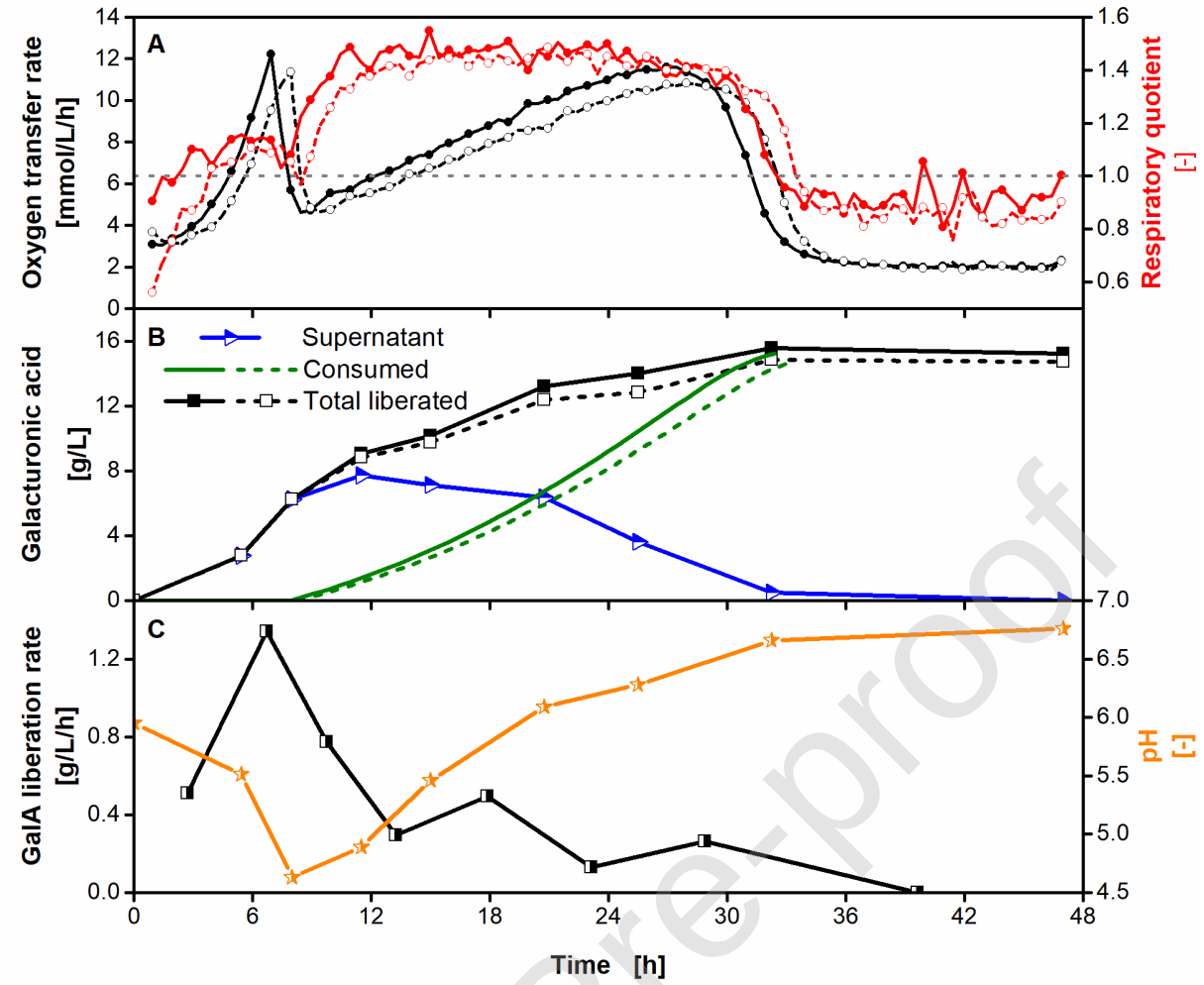

Fig. 11. Galacturonic acid liberation rate during co-fermentation of AtPgaX (fungal exo-polygalacturonase) and AaPgu1 (fungal endo-polygalacturonase) overexpression strains (inoculation ratio 5:1) on polygalacturonic acid. The strains were grown on a mixture of glucose (4 g/L) and polygalacturonic acid (20 g/L, purity 85%) as carbon sources. **A**, Oxygen transfer rate and respiratory quotient of biological duplicates (continuous and dashed lines, identical data set to Fig. 10C) **B**, Measured galacturonic acid concentration in the supernatant and consumed galacturonic acid, calculated from the overall consumed oxygen. End of polygalacturonic acid consumption was defined by the RQ drop below 1. Total liberated galacturonic acid equals the sum of both quantities. **C**, Calculated galacturonic acid liberation rate (mean of biological duplicates) in comparison to the offline determined pH. Culture conditions: modified Verduyn mineral medium, 0.2 M MOPS, initial pH 6.0, 250 mL flask, filling volume 20 mL, shaking frequency 300 rpm, shaking diameter 50 mm, initial OD_{600} = 0.5 (AB33P5ΔR/AtPgaX) or 0.1 (AB33P5ΔR/AaPgu1), T = 30 °C.

Table 1. DNA oligonucleotides used in this study.

Designation	Nucleotide sequence (5´- 3´)
oMB425	ACAGCTCTTCCGTGCATTTAAATACCTCGAAGCACAACGTACG
oMB426	ACAGCTCTTCCGGCCCACCCGAGGCACCGTCTTTATGC
oMB427	ACAGCTCTTCCCCTATGGCCTGCCTTTTGCTGGTTGG
oMB428	CGCGCTCTTCCGACATTTAAATACCCGACAATTTGATGTTGG
oMF502	ACGACGTTGTAAAACGACGGCCAG
oMF503	TTCACACAGGAAACAGCTATGACC

Table 2. *U. maydis* strains used in this study.

Strains	**Relevant genotype, Resistance**	**UMa[1]**	**Reference**	**Plasmid transformed**	**Manipulated locus[2]**	**Progenitor (UMa)[1] [Reference]**
AB33P5ΔR	*FRT5[um04400 Δ] FRT3[um11908Δ] FRT2[um00064 Δ] FRTwt[um02178Δ] FRT1[um04926Δ]* PhleoR	1391	(52)	detailed strain description in Sarkari *et al*. 2014 (52)	*ip (cbx), umag_04400, umag_11908, umag_00064, umag_2178, umag_04926*	AB33 (62)
AB33P5ΔR /UmPgu1	*FRT5[um04400 Δ] FRT3[um11908Δ] FRT2[um00064 Δ] FRTwt[um02178Δ] FRT1[um04926Δ]* P*02510*::*umag_02510*::P*oma*::*um02510* PhleoR, NatR	2030	This study.	pDest_Poma:umag_02510_NatR (pUMa2822)	*umag_02510*	AB33P5ΔR (UM1391) (52)
AB33P5ΔR /AtPgaX	*FRT5[um04400 Δ] FRT3[um11908Δ] FRT2[um00064 Δ] FRTwt[um02178Δ] FRT1[um04926Δ]* ip^r [P_{oma}*AtPgaX:SHH]* ip^s PhleoR, CbxR	2106	(54)	pRabX1_Poma_pgaX_SHH_CbxR (pUMa3108)	*ip (cbx)*	AB33P5ΔR (UM1391) (52)
AB33P5ΔR /AaPgu1[3]	*FRT5[um04400 Δ] FRT3[um11908Δ] FRT2[um00064 Δ] FRTwt[um02178Δ] FRT1[um04926Δ]* ip^r [P_{oma}*AaPgu1:SHH]* ip^s PhleoR, CbxR	2416	This study.	pRabX1_Poma_AaPgu1_SHH_CbxR (pUMa3403)	*ip (cbx)*	AB33P5ΔR (UM1391) (52)
AB33P5ΔR /PcPeh1[4]	*FRT5[um04400 Δ] FRT3[um11908Δ] FRT2[um00064 Δ] FRTwt[um02178Δ] FRT1[um04926Δ]*	2402	This study.	pRabX1_Poma_Peh1-SHH-Cts1_CbxR (pUMa3401)	*ip (cbx)*	AB33P5ΔR (UM1391) (52)

	ip^r [P$_{oma}$PcPeh1:SHH: cts1] ip^s PhleoR, CbxR					
AB33P5ΔR /KpPguB[4]	*FRT5[um04400 Δ] FRT3[um11908Δ] FRT2[um00064 Δ] FRTwt[um02178Δ] FRT1[um04926Δ] ip^r [P$_{oma}$KpPguB:SHH: cts1] ip^s* PhleoR, CbxR	2401	This study.	pRabX1_Poma_ PguB-SHH- Cts1_CbxR (pUMa3400)	*ip (cbx)*	AB33P5ΔR(UM1391) (52)

[1] Internal strain collection number
[2] Sequences available at the National Center for Biotechnology Information (NCBI) or EnsemblFungi (web reference 4)
[3] The intrinsic signal peptide encoding sequences of the enzymes were kept
[4] The intrinsic signal peptide encoding sequences predicted by SignalP 4.1 were removed to allow for unconventional secretion (web reference 7)